

AD-A165 670

A STUDY OF GROUP-TYPE SINGLE-PHASE UNIDIRECTIONAL SAW  
TRANSDUCERS ON LINB. (U) ROYAL SIGNALS AND RADAR  
ESTABLISHMENT MALVERN (ENGLAND) M F LEWIS JUN 85

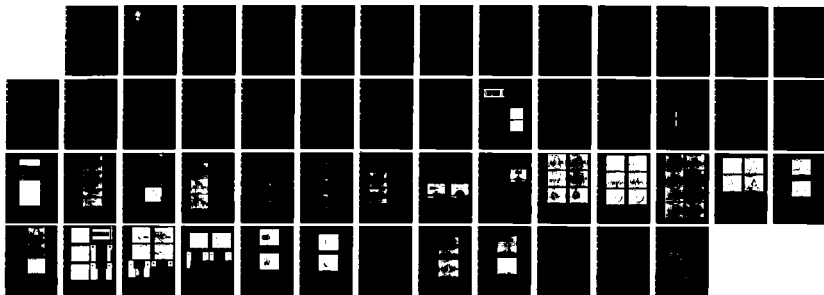
1/1

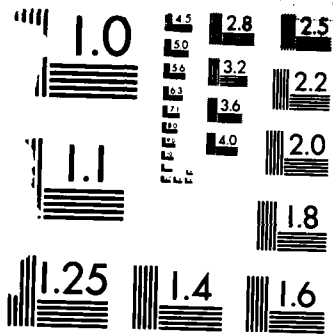
UNCLASSIFIED

RSRE-NEMO-3833 DRIC-BR-98351

F/G 28/2

ML





MICROCOPY RESOLUTION TEST CHART  
NATIONAL BUREAU OF STANDARDS 1963-A

UNLIMITED

BR98351

2



RSRE  
MEMORANDUM No. 3833

ROYAL SIGNALS & RADAR  
ESTABLISHMENT

AD-A165 670

A STUDY OF GROUP-TYPE SINGLE-PHASE UNIDIRECTIONAL  
SAW TRANSDUCERS ON  $\text{LiNbO}_3$  AND QUARTZ

Author: M F Lewis

RSRE MEMORANDUM No. 3833

DTIC FILE COPY

PROCUREMENT EXECUTIVE,  
MINISTRY OF DEFENCE,  
RSRE MALVERN,  
WORCS.

DTIC  
ELECTE  
MAR 24 1966  
S D E

UNLIMITED

86 3 21 058

ROYAL SIGNALS AND RADAR ESTABLISHMENT

Memorandum 3833

TITLE: A STUDY OF GROUP-TYPE SINGLE-PHASE UNIDIRECTIONAL  
SAW TRANSDUCERS ON  $\text{LiNbO}_3$  AND QUARTZ

AUTHOR: M F Lewis

DATE: June 1985

SUMMARY

This Memorandum describes a development of the SPUDT (Single Phase Unidirectional Transducer) concept. The new design employs 'sampled' transducers to allow the introduction of reflector banks within the transducers. The fabrication of such devices requires a single stage of photolithography. Prototype devices have shown very encouraging passband characteristics with an insertion loss of less than 3 dB on  $\text{LiNbO}_3$  at 100 MHz, and less than 6 dB on quartz at 400 MHz. In each case the amplitude response is essentially ripple-free, and the phase characteristic agreeably linear.

Accession For	
NTIS GRA&I	<input checked="" type="checkbox"/>
DTIC TAB	<input type="checkbox"/>
Unannounced	<input type="checkbox"/>
Justification	
By _____	
Distribution/	
Availability Codes	
Avail and/or	
Dist	Special
A-1	



Copyright  
C  
Controller HMSO London  
1985

MEMORANDUM NO 3833

A STUDY OF GROUP-TYPE SINGLE-PHASE UNIDIRECTIONAL SAW TRANSDUCERS ON  $\text{LiNbO}_3$   
AND QUARTZ

M F Lewis

LIST OF CONTENTS

- 1 Introduction
  - 2 A Review of Conventional IDTs and a Preliminary Description of the Group-Type SPUDT
  - 3 Preliminary Experiments on a Test Group-Type SPUDT Device
  - 4 First 2-port Group-Type SPUDT Devices on  $\text{LiNbO}_3$ 
    - 4.1 Devices comprising transducers 'A'
    - 4.2 Devices comprising transducers 'D'
    - 4.3 Devices comprising transducers 'D' and 'E'
  - 5 Group-Type SPUDT Devices on ST-Quartz
    - 5.1 Measurements on devices employing 1500 Å Al
  - 6 Group-Type SPUDT Devices on AT-Quartz
  - 7 Conclusion
- References

LIST OF APPENDICES

- 1
- 2
- 3

## 1 INTRODUCTION

In the past numerous designs of surface acoustic wave (SAW) bandpass filter have been reported based on a variety of interdigital transducer (IDT) geometries<sup>(1)</sup>. Such devices offer the systems engineer a number of attractive features: SAW filters are small, cheap, rugged, reproducible, passive, planar components covering the range from 10 MHz to >1 GHz and displaying excellent group delay and stop-band rejection characteristics. Most such filters incur an insertion loss of order 20 dB, since by accepting this loss; (i) the design procedure is simplified, (ii) the effect of the spurious triple transit signal is made minimal, and (iii) matching to the external circuit is non-critical. At IF such a loss is often acceptable as it does not degrade the signal/noise ratio significantly, and the loss itself is readily made good by means of an additional stage of IF amplification. It is, however, self-evident that filters with a lower loss are preferable, and in some applications they are vital (eg for front-end filtering, and in applications demanding minimum size and power consumption). To this end SAW research workers have devised several techniques for reducing the loss of SAW filters to a few dBs<sup>(2)</sup>. These include multistrip coupler-based unidirectional IDTs<sup>(3)</sup>, multiphase IDTs<sup>(4)</sup>, two-port resonators (Refs 5-7), interdigitated IDTs<sup>(8)</sup>, a family of 'ring' filter duplicated arrangements<sup>(9,10)</sup>, and the travelling wave transducer<sup>(11)</sup>. Most of these devices incur one or more penalties, eg increased substrate area, more complex fabrication and matching circuitry, and/or a restricted range of realisable filter characteristics. A recent addition to this list of low-loss filter techniques is the structure of Hartmann et al<sup>(12,13)</sup> which reduces the 3 dB bidirectionality loss of each IDT by incorporating an (offset) reflector array to enhance the required forward wave at the expense of the unwanted backward wave. The experimental arrangement used by Hartmann et al to demonstrate the principle comprised an array of gold reflectors deposited on to the aluminium IDTs in a second metal evaporation process.

In this Memorandum we describe a novel arrangement whereby the reflector bank is generated from the same metal and in the same photolithographic process as the IDT itself, thereby simplifying the fabrication and relieving the problem of alignment between the reflectors and the IDTs. This new design also enjoys a number of secondary advantages, eg it can employ various SAW reflection mechanisms (mass-loading, piezoelectric shorting, topographical) singly or in combination, and it can employ reflectors of arbitrary dimensions, in particular reflectors of any width. The only significant disadvantage foreseen to date concerns the limited out-of-band rejection achievable as a result of the spurious passbands of each IDT; these result from the IDT 'sampling' process necessary to introduce the reflector banks. Nevertheless it should be noted that various SAW devices (principally oscillators) already employ such 'sampled' or 'ladder' transducers with empty gaps between the active sections, and in such cases the incorporation of unidirectional reflector banks in these spaces incurs no additional penalty of any consequence.

We would also like to emphasise another potentially beneficial aspect of low-loss SAW filters which has not received mention to date. This is their eminent suitability for use in cascade, ie connected in series. While such an arrangement has occasionally been advocated for conventional SAW filters to enhance their stopband rejection, the high loss/intermediate stages of amplification detract greatly from the attraction of this SAW approach. By contrast, with modern low-loss SAW techniques such as the one described in this Memorandum, it is possible to provide an enhanced rejection, and still have a significantly improved insertion loss relative to a conventional SAW filter. This is

demonstrated in Appendix 1 for some particular low-loss filters the author had available at the time of writing. Notice that the series-connection of identical filters demonstrated in Appendix 1 is the worst possible case as it maximises the in-band ripple and out-of-band rejection; staggering the individual responses will enhance the performance significantly and a preliminary demonstration of this is also included in Appendix 1. In effect then, the low-loss capability not only opens new avenues to the use of SAW devices (eg as front-end filters) but also adds a new degree of freedom to the designer, namely the ability to cascade frequency responses. All conventional (eg apodised) SAW bandpass filter designs essentially comprise elementary filters in parallel, as is evident from Tancrrell and Holland's analysis procedure for such devices<sup>(14)</sup>. In many cases the individual low-loss SAW filters described here are sufficiently small that two or more can easily be made on one substrate and connected directly, or via external components such as tuning inductors.

In the following sections we describe the construction and principles of operation of the new device, the results of various preliminary measurements on a simple test group-type SPUDT structure, and a comparison of this behaviour with a simple time-domain (impulse-response) model. In the later sections we describe the design and performance of low-loss devices employing piezoelectric shorting on LiNbO<sub>3</sub>, and mass-loading on quartz. To date the results have been most encouraging, and bode well for the future of a new generation of very low loss SAW devices.

## 2 A REVIEW OF CONVENTIONAL IDTs AND A PRELIMINARY DESCRIPTION OF THE GROUP-TYPE SPUDT

A conventional SAW IDT comprises two sets of interpenetrating metallic electrodes deposited on a piezoelectric substrate. Two commonly used symmetric periodic versions are shown schematically in Figure 1, the split-finger version being used to reduce internal reflections, eg due to the mass of the electrodes. The application of a sinusoidal voltage,  $V$ , across the busbars causes a spatially and temporally-periodic deformation of the piezoelectric substrate within the overlap region of the transducer fingers. Assuming that the aperture,  $A$ , is much greater than the SAW wavelength,  $\lambda$ , this causes a plane SAW to propagate in each direction (ie to the LHS and RHS) away from each period of the transducer. If in addition the frequency,  $\omega$ , is chosen such that  $\lambda = p$ , then the wavelets generated by each period add constructively to generate an intense net SAW output in each direction. At other frequencies the interference of these wavelets is less constructive and the net SAW output correspondingly weaker. When driven from a low-impedance electrical source, the overall frequency response of an IDT comprising  $N$  periods is identical to that of an optical diffraction grating comprising  $N$  slits, ie is of the sinc-function form with a fractional bandwidth  $\sim 1/N$ . This is most readily derived by considering each period of the IDT to be a  $\delta$ -function source of SAW, when the impulse response becomes

$$h(t) \propto \sum_{n=1}^N \delta(t - n\tau)$$

where  $\tau = p/V$ ,  $V$  = SAW velocity. The frequency response is given by the Fourier Transform of  $h(t)$ ,

$$H(f) = \int_{-\infty}^{\infty} h(t) \exp(-j2\pi ft) dt \propto \sum_{n=1}^N \exp(-j2\pi fn\tau)$$

This expression is identical in form to that for an optical diffraction grating<sup>(15)</sup> and so leads to the same sinc-function frequency response, and is readily visualised with the help of phasor diagrams (Ref 15, Figure 17H). In Appendix 2 this  $\delta$ -function impulse response model is extended to the topic of this Memorandum, the group-type SPUDT.

Regardless of the frequency, SAW of equal intensity are excited in each direction as a result of the bilateral symmetry of the structure of Figure 1. The IDT as a whole may therefore be regarded as a symmetrical 3-port junction, with one electrical and two identical acoustic ports. One consequence of this is that if the IDT is otherwise lossless, it is impossible to match all 3 ports simultaneously<sup>(16)</sup>. This leads to the well-known problem of triple-transit signals in SAW devices employing IDTs. The problem has been recognised for many years, and described by various workers<sup>(2,17)</sup>, and the author has recently given a simplified treatment of the problem based on symmetry arguments alone (Ref 18). The solution to this problem adopted by most SAW device manufacturers to date is to mismatch the transducers electrically to a sufficient degree that the triple transit signal is negligible relative to the required single-transit signal, and this typically results in an overall insertion loss of 20-30 dB. (It is worth mentioning that this procedure of mismatching by the omission of tuning circuitry is simple and convenient, but does not result in the maximum possible triple-transit suppression for a given insertion loss.) Many modern systems, however, would benefit from lower insertion losses, and a wide variety of approaches to lower loss have been described in the literature<sup>(2-13)</sup>. The SPUDT<sup>(12,13)</sup> is a recent version which breaks the symmetry of the simple IDT of Figure 1 by incorporating an offset reflector array within the IDT itself, Figure 2. A previous device employing a similar principle is the SAW resonator (Refs 5-7) which employed (offset) reflector banks externally to the transducers. In Figure 2, acoustic reflectors caused by the gold have been shown theoretically and experimentally to enhance the forward wave at the expense of the backward wave<sup>(12,13)</sup>. However this original device possesses several practical disadvantages and to overcome these the author has investigated the group-type SPUDT shown schematically in Figure 3. This comprises two 'ladder' transducers with (offset) reflector banks in the spaces between the active 'rungs' of each ladder. Such ladder IDTs have been used in the past in a variety of applications. The attraction of Figure 3 is immediately apparent - the reflector array is fabricated in the same photolithographic process as the transducers, and the unidirectional transducers occupy a space only marginally, if any, greater than their bidirectional counterparts.

Hartmann et al<sup>(12,13)</sup> have used a coupling-of-modes (COM) theory to describe the operation of a conventional IDT with a superimposed reflector array. An important result to emerge from this theory is that for optimum unidirectionality the individual reflectors should be offset from the transducer fingers by  $\pm \lambda/8$  where  $\lambda$  is the SAW wavelength at the centre frequency. In a recent paper the author has shown that the same result obtains for the ladder arrangement of Figure 3<sup>(19)</sup>. Rather than repeat the content of these papers, the latter is included here as Appendix 3. While on this topic, it is also interesting to note that the original COM approach, as formulated by Hartmann et al, automatically reproduces the behaviour of a "crossed-field" model of a conventional transducer<sup>(12)</sup>. It would be of interest to investigate how this should be modified/generalised to produce other behaviours, principally that of the "in-line" model.

Before leaving this section we would like to emphasise that the development of the SPUDT or any other unidirectional transducer infers two immediate benefits on devices employing it. Firstly, it makes very low insertion losses possible, and secondly it eliminates the amplitude and phase ripple caused by triple transit signals in conventional SAW devices. This arises because the transducers ideally become 2-port devices. This latter advantage is often at least as important as the former\*. It does, however, impose stringent conditions on the electrical matching to the external circuit, for if a 2-port junction is mismatched, any energy not coupled out is totally reflected, causing an even more severe triple-transit problem than in a conventional device.

### 3 PRELIMINARY EXPERIMENTS ON A TEST GROUP-TYPE SPUDT DEVICE

As shown in Figure 2 the original SPUDT device employed SAW reflections caused by the mass-loading of an array of gold strips on a quartz substrate. A simpler approach was adopted here, namely to employ reflections (predominantly) due to the piezoelectric-shorting effect of a metal strip on the strongly piezoelectric material, LiNbO<sub>3</sub>. Such reflections have often been studied and used in the past<sup>(20,21)</sup> and are fairly well understood<sup>(21)</sup>. A rough model of the reflection process is simply to assume an (amplitude) reflection coefficient,  $a$ , at each edge of the strip, where

$$a = \frac{Z_1 - Z_2}{Z_1 + Z_2} \approx \frac{\Delta V}{2V} \approx \frac{k^2}{4} \approx \frac{1}{80} \quad \text{for YZ-LiNbO}_3 \quad (1)$$

Here the acoustic impedance  $Z = \rho V$  where  $\rho$  is the mass density, while  $V_1$  and  $V_2$  are the SAW velocities on the free and metallised substrates.  $\Delta V = V_1 - V_2$  is related to the piezoelectric coupling constant of the material/cut by  $k^2 \approx 2\Delta V/V$ <sup>(17)</sup>. This argument is by analogy with bulk-wave devices and is not in any way rigorous for the SAW device. (For example, the bulk-wave problem is one-dimensional, while the SAW problem is 2-dimensional in view of the decay of the SAW disturbance into the substrate in a distance of order one wavelength  $\lambda$ . Further the simple model does not predict the correction variation of reflection coefficient with strip width, Ref (21), Figure 3.) The advantage of this simplified approach is that it is easily visualised and gives an answer of the correct order of magnitude. The amplitude reflection coefficient of a complete strip is therefore  $2a \sim 1/40$  if the width is  $\lambda/4$ , when the reflections from the two edges add coherently. Thus we may expect a considerable degree of unidirectionality from such a device if it incorporates  $\sim 40$  reflectors per transducer. It is shown in Ref (12) that a device comprising two such transducers could show a loss of only 1 dB, and 37 dB triple-transit suppression, a dramatic improvement over a conventional SAW device.

The first RSRE test pattern was designed in accordance with the discussion above and employed a single unidirectional test transducer with 5 'rungs' of 2 finger pairs/rung, and a rung-to-rung spacing of  $8\lambda$ . In addition it contained 5 ( $\lambda/8$ -offset) reflector banks, each containing 10 reflecting strips of width  $\lambda/4$ . A photograph of part of the device mask is shown in Figure 4 together with one of the 4 identical conventional tests IDTs that

---

\*In fact it is common practice to match low-loss SAW devices for minimum triple-transit effects, rather than for the lowest insertion loss, although these conditions should not be very different if the device is well-designed.

surround the unidirectional transducer, and which enable a variety of useful measurements to be undertaken. The acoustic aperture of each transducer is  $100 \lambda$ , as is commonly used in such devices. The acoustic wavelength was chosen as  $34.5 \mu\text{m}$ , giving an operating frequency of 100 MHz on YZ-LiNbO<sub>3</sub>. The overall arrangement is shown schematically in Figure 4, and is labelled pattern 'A' on RSRE mask AW 1724. This mask also contained pattern 'C', which is identical in design but omits the reflector banks, and was included for comparison with 'A'.

In Figure 5 we compare the basic characteristics (measured in a  $50 \Omega$  system) of the untuned test unidirectional transducer 'A' in the forward and reverse directions, and also include the response of 'C' (which is of course the same in both directions). As anticipated above, a comparison of the upper two traces of Figure 5 confirms a useful degree of unidirectionality, amounting to about 5 dB difference between the forward and reverse directions at the centre frequency. As in the case of SAW resonators on YZ-LiNbO<sub>3</sub>, the forward direction corresponds to the reflectors being displaced  $\lambda/8$  towards the other transducer. This does not necessarily apply to other substrates, some of which will operate in the opposite sense. However, as shown in Appendix 3, all substrates will operate optimally one way or the other for an offset of  $\pm \lambda/8$ . In Figure 5, pattern 'C' shows an intermediate loss, and also a small frequency shift of about +0.3 MHz, which arises because the slowing effect of the metal reflector banks is absent in this pattern. This shift varies slightly from device to device due to fabrication variations, eg metal thickness, and mark/space ratio variations in photolithography.

All patterns show some in-band ripple due to reflections between the transducers (principally the triple-transit signal). This problem becomes more severe when the transducers are tuned and matched (to the  $50 \Omega$  input and output circuits), Figure 6, and illustrates one of the principal problems with conventional SAW devices. As discussed earlier this triple-transit problem is one of the deleterious effects minimised in a fully-optimised unidirectional SAW device, and this is confirmed by the behaviour of the devices described in later sections. In the lowest photograph of Figure 6 we compare the forward and reverse responses over a wide band. It will be noted that the reflectors have a negligible effect outside the main passband, a result which is explained later. This result is agreeable as it means that no special precautions are necessary to ensure a useful degree of out-of-band rejection when designing such SAW devices, unless extreme out-of-band rejection is required.

A further series of tests has been conducted on this simple unidirectional transducer 'A' for comparison with theory. In Figure 7 the basic passband responses are illustrated, the difference between these and earlier results being that a low impedance ( $10 \Omega$ ) was incorporated across the transducer to facilitate comparison with the theoretical responses derived from an impulse-response model (and shown to the right of the measurements). The basis of the impulse-response model is outlined in Appendix 2. Figure 8 shows the corresponding results for the phase response. The data plotted are actually the phase deviations relative to the response of the comparison device 'C', and were made with a storage normaliser attachment to the HP 8505A network analyser.

Figures 9 and 10 show the corresponding measurements and calculations for a more symmetrical structure obtained by disconnecting one 'rung' of the ladder transducer by means of a laser burner. The resulting structure is shown schematically at the tops of Figures 9 and 10. Evidently there is again a respectable degree of agreement between measurement and the calculations.

The final measurements made on the test unidirectional transducer 'A' is illustrated in Figure 11, and was designed to confirm the anticipated behaviour of the reflector banks, and to obtain an estimate of the reflection coefficient. To this end the ladder transducer itself was short-circuited electrically. As it comprises split-finger transducer sections this has the effect of essentially removing it from the substrate as far as the SAW are concerned, enabling the behaviour of the reflectors to be measured without complication. The far LHS monitoring transducer was impulsed, and the reflections and transmission measured in the time and frequency domains simultaneously using the well-established RSRE technique show in Figure 12. As expected the reflected SAW comprise 5 RF bursts corresponding to the 5 reflector banks, and have a frequency spectrum of essentially sinc-function form with a width half that of the main passbands of Figures 5-7. This arises because their impulse response has double the time-duration of the transducer's impulse response, ie because the waves travel to the reflectors and back. This result, and a similar one concerning the overall impulse response of an IDT containing reflectors (Appendix 2), explain why the reflectors only have a significant effect in the main passband, Figure 6.

The transmitted response, Figure 11(b), shows the much broader frequency response characteristic of the 5-finger-pair monitoring transducers, with a relatively narrow notch caused by the reflections. Once again a small frequency shift is evident between the responses of the monitoring IDTs and the reflections from the transducer 'A', due to the different metallisation patterns. An approximate value of the amplitude reflection coefficient is 0.12 per bank, or 1.2% per reflector. This is about one half of the value suggested earlier. However such a difference is not unexpected, and the measured result is within the range of values given by Paige et al<sup>(21)</sup>. This experimental value of 1.2% per strip was used in the impulse response calculations of Figures 7 to 10, and evidently produces satisfactory agreement with experiment.

In concluding this section we can say that all the measurements presented are in good qualitative agreement with expectations, and suggest that the group-type SPUDT of Figure 3 offers similar interesting possibilities to the original SPUDT design for producing low-loss SAW devices.

#### 4 FIRST 2-PORT GROUP-TYPE SPUDT DEVICES ON $\text{LiNbO}_3$

In view of the results of section 3, a new mask was designed to test the behaviour of 2-port group-type SPUDT devices. This is RSRE artwork AW 1728 (MFL Book 11c, page 20) and contains 3 basic test patterns. The first pattern contained 2 transducers 'A' which are of identical design to the earlier pattern 'A' of AW 1724, but with the aperture reduced from  $100 \lambda$  to  $70 \lambda$  to provide a closer match to  $50 \Omega$  when series tuned. This pattern could be measured with the transducers 'front-to-front' or 'back-to-back' (for comparison).

The second pattern contained transducers 'D', which were similar to 'A' but comprised 10 rungs and 10 reflector banks (rather than 5 of each in 'A'). These were of aperture  $70 \lambda$ , and could also be measured 'front-to-front' or 'back-to-back'.

(Note: If necessary this pattern could be lasered down to a smaller number of rungs by laser burning the metal connections and adding absorber to eliminate reflections.)

In designs 'A' and 'D' spurious responses were to be anticipated since each transducer of a pair contained identical 'sampled' or ladder transducers. (These spurious are visible in Figure 6c, for example.) To avoid this effect in a prototype bandpass filter a third transducer was employed, called 'E', whose design was chosen to minimise the overlap of its spurious passbands with those of transducer 'D'. Transducer 'E' comprised 10 'rungs' of 2 finger pairs per rung,  $10 \lambda$  rung-to-rung spacing, and each reflector bank contained 14 reflectors. This design also aimed to maintain an approximate balance between the fractions of 'D' and 'E' metallised to avoid significant relative frequency shifts.

Detailed measurements have been undertaken on these devices in the time and frequency domains, and are summarised in the series of photographs comprising Figures 13 to 15 together with the notes below (Reference MFL BK 11F, page 81).

#### 4.1 DEVICES COMPRISING TRANSDUCERS 'A'

The transducers were series tuned with inductors of 150 nH to give them a real impedance close to  $50 \Omega$  at the centre frequency; Figures 13(c) and (f) show this for the forward and reverse pairs respectively. In each case the other transducer was also tuned and loaded with  $50 \Omega$ . Figures 13(a) and (b) show that in the forward direction the loss is a 'respectable' 5 dB, but a significant triple transit signal remains. It is apparent from Figures 13(d) and (e) that the back-to-back arrangement shows a higher loss and distorted passband. The overall conclusion is that the transducers 'A' exhibit a modest directionality but not enough to produce a very low forward loss or very high reverse loss. Consistent with this is the remaining high level of the triple transit signal. It may be noted that this triple transit signal could probably be eliminated by mismatching the transducers<sup>(12,13)</sup> but would result in an even higher insertion loss.

#### 4.2 DEVICES COMPRISING TRANSDUCERS 'D'

In this device (as in the device containing transducers 'D' and 'E') it was found better to shunt tune each transducer with about 100 nH in order to produce a smooth passband. The reason for this is believed to lie in the fact that the transducer's static capacitance,  $C_0$ , has a reactance,  $jX$ , of modulus about  $50 \Omega$ , ie about the same as the parallel radiation resistance,  $R_p$ ; in these circumstances the usual derivation of the series radiation resistance,  $R_a$ , is invalid since it assumes  $R_p \gg X \gg R_a$ . In the present circumstances the shunt equivalent circuit is 'better' than a series one, a contentious statement that can be justified by relating the strength of the acoustic waves excited to the actual voltage across the transducer's terminals. Figure 14 shows a series of measurements on devices comprising transducers 'D' and may be compared with Figure 13 on devices containing transducers 'A'. It is immediately apparent that this arrangement shows greater directionality, with a low-loss and absence of passband ripple in the forward pair, and a deep null at the centre frequency of the reverse pair. Consistent with this is the observation that the  $S_{11}$  measurement in Figure 14(c) is very sensitive to the matching/loading of its 'mate' transducer, while in Figure 14(f) it is rather insensitive, the input transducer being strongly directional and sending most of its output straight into the end absorber!

### 4.3 DEVICES COMPRISING TRANSDUCERS 'D' AND 'E'

The behaviour of this pattern is shown in Figure 15 and is basically very similar to the pattern comprising two transducers 'D'. The principal difference lies in the out-of-band rejection; it is evident from Figure 15(d) that the staggered design 'D' + 'E' has suppressed the spurious passbands at  $\sim 75, 87.5, 112.5$  and  $125$  MHz in Figure 14(b). In truth a greater degree of suppression will usually be required in practice and this must be built into the design of the transducers, eg by employing more active finger pairs per rung and/or smaller rung-to-rung separations,  $m\lambda$ , since the spurious occur at  $f_0 (1 \pm n/m)$  where  $f_0$  is the centre frequency and  $n$  is an integer. Another aid to improved out-of-band rejection is to employ low-loss devices in series, as discussed in Appendix 1. Yet another possibility is to employ a conventional bidirectional IDT in conjunction with 2 outer SPUDTs.

Numerous other measurements have been undertaken in the course of this work. Below we describe three results of particular interest. These concern (i) the behaviour of the reflectors at the third harmonic response (which is present because the basic IDT comprises split-fingers), (ii) the behaviour of a group-type SPUDT device employing electrically-shortened rather than isolated reflecting strips, and (iii) the performance of group-type SPUDT devices on  $128^\circ \text{LiNbO}_3$ .

#### (i) Third-Harmonic Operation

The possibility of using the third harmonic response of split-finger SAW devices is of practical interest, principally to provide low-loss devices for use as front-end filters at UHF and low microwave frequencies. We have therefore examined some of the devices described above at their third harmonic response ( $\sim 300$  MHz). The principal observation is that any unidirectional properties at this frequency are very weak, a result consistent with Paige et al<sup>(21)</sup>, who show that the reflection coefficient per strip goes through zero for a width  $\sim 0.8 \lambda$ . Our observations are presented in Figure 16 and show that the dramatic difference between the forward and reverse devices at the fundamental frequency is very marginal at the third harmonic. One might expect a weak reverse unidirectionality at the third harmonic because an offset of  $\lambda/8$  at the fundamental is equivalent to  $3\lambda'/8$  at the third harmonic which, in reflection (twice the pathlength) is equivalent to  $-\lambda'/8$ . Some devices do seem to show this, but the overall effect is too weak to be quantified. Differences between devices probably arise from mark/space ratio variations in fabrication and it should also be noted that according to Paige<sup>(21)</sup> the reflection coefficient changes sign at a width  $\sim 0.8 \lambda$ . A useful degree of unidirectionality at the third harmonic can probably be achieved by reducing the widths of the reflectors to  $\sim 0.5 \lambda'$  (Ref (21), Figure 3) and a demonstration of this effect has been made by over-etching one of our devices in the photolithographic process.

(ii) Devices employing Electrically-Shorted Reflector Banks

In an early paper, Dunnrowicz et al<sup>(20)</sup> observed a reversal in the sign of the reflection coefficient from a bank of metallic strips on YZ-LiNbO<sub>3</sub> when the strips were electrically shorted to form a 'grid-iron' pattern. Since this option is one available to the group-type SPUDT transducer designer we have investigated it by modifying our artwork AW 1728. This was done by adding shorting strips by hand to a blown-up copy, and subsequently reducing it photographically to produce a new artwork, AW 1728/M (MFL BK 11D, page 28). Unfortunately the resulting mask is of poor quality (eg showing barrel distortion) and operates at a fundamental frequency of about 187 MHz on YZ-LiNbO<sub>3</sub>. Measurements on untuned devices containing transducer patterns 'D' and 'E' leave no doubt, however, that the sense of unidirectionality is reversed, Figure 17. No further work was undertaken to optimise the performance of these devices because of their poor quality. Nevertheless these results confirm that electrically-shortened reflector strips are a viable option to the SPUDT designer. They evidently have a strong reflection coefficient, and could presumably be earthed, possibly offering minor practical advantages over electrically isolated strips.

(iii) Devices on 128° LiNbO<sub>3</sub>

This is increasingly being used as an alternative to YZ-LiNbO<sub>3</sub>, eg in TV filters, and has two advantages over YZ-LiNbO<sub>3</sub>: (a) a higher piezoelectric coupling constant,  $k^2$ , and (b) it produces less spurious bulk waves. It is therefore of interest as a potential substrate for low-loss group-type SPUDT devices. A few measurements have been made on such devices produced from artwork AW 1728 and, as expected, have produced results basically similar to YZ-LiNbO<sub>3</sub> but at a frequency about 14% higher due to the higher SAW velocity on 128° LiNbO<sub>3</sub>. In Figure 18(a) we show a measurement on a device comprising transducers 'D' and 'E', each being shunt-tuned. This somewhat distorted result is indicative of too high a coupling so the device was reduced to 7 rungs per transducer by lasering the outer 3 rungs of each, and covering the unwanted rungs and reflectors with absorber. The resulting response of Figure 18(b) is both cleaner and of appreciably greater bandwidth than the YZ-LiNbO<sub>3</sub> devices. This latter aspect is an important one, and suggests that 128° LiNbO<sub>3</sub> (and other high-coupling SAW or related-wave cuts/materials) warrant further investigation (Reference MFL Book 11D, pp 20-25).

In view of these findings it was decided to investigate the behaviour on 128° LiNbO<sub>3</sub> of the previously described device pattern comprising two transducers of design 'A'. By matching each IDT to 50  $\Omega$  with a shunt inductor (~ 300 nH) and a series inductor (~ 150 nH) an excellent response was obtained with 3.7 dB loss, and a smooth passband, and linear phase characteristic, Figure 18(c). In conclusion it appears that the 128° LiNbO<sub>3</sub> substrate offers the advantage of a greater fractional bandwidth, the device of Figure 18(c) showing a 3 dB bandwidth of 2%.

## 5 GROUP-TYPE SPUDT DEVICES ON ST-QUARTZ

Having proved the principle of the group-type SPUDT on  $\text{LiNbO}_3$  it was obviously of interest to extend the investigation to quartz, with its advantage of temperature-stability, which is of especial importance in narrow band devices. Such devices would complement the low-loss but very narrow band SAW resonator (Refs 5-7). As the piezoelectric coupling constant,  $k^2$ , of quartz is very much lower than that of  $\text{LiNbO}_3$  it was necessary to employ another SAW reflection mechanism. An obvious choice is the mass loading/ topographical mechanism. We chose to use reflections from aluminium strips rather than gold<sup>(12)</sup> to avoid the extra processing involved, although we may note that devices employing gold for both transducers and reflectors form a viable alternative, especially at lower frequencies. The use of gold may also offer secondary advantages like improved ageing through its immunity to oxidation.

The test patterns on quartz were implemented in RSRE artwork AW 1729 (MFL Book 11c, page 30) and employed six comparison patterns:

- (1) Comprised two ladder transducers using conventional finger widths and gaps of  $\lambda/4$  (NB: NOT split-fingers).
- (2) This was similar, but also incorporated antireflection 'blooming' strips described earlier by the author<sup>(22)</sup>.
- (3) This was similar to (2), but additionally incorporated many unidirectional reflecting strips, Table 1.
- (4) This was similar to (3), but employed fewer strips, Table 1.
- (5) This was somewhat similar to (3) but attempted to combine the blooming and unidirectional reflecting strips into one equivalent bank per period of the structure. The offset was a weighted average of the  $\lambda/8$  and  $\lambda/4$  offsets, Table 1.
- (6) This was similar to (5), but employed less combined-purpose strips, Table 1.

Full details of these patterns are given in Table 1, and photographs of sections of the devices are included in Figures 19 to 21. As in the case of the resonators described by Marshall<sup>(7)</sup>, the reflectors were displaced  $\lambda/8$  away from the other transducer. This is the opposite sense to  $\text{LiNbO}_3$ .

The centre frequency was chosen as 400 MHz on ST-quartz and the design described is typical of many requirements for use in FM oscillators encountered by the author in the past. As in the  $\text{LiNbO}_3$  devices described earlier, the designs of the individual transducers were arranged to overlap only at the fundamental frequency (400 MHz), and a careful metallisation balance was maintained in all designs (Table 1) to ensure tracking of the centre frequencies of the pairs of transducers in each device.

The metal thickness required to provide a similar degree of reflection coefficient and unidirectionality to the  $\text{LiNbO}_3$  devices described earlier was estimated from the measurements of Marshall<sup>(7)</sup>. According to Marshall the amplitude reflection coefficient per edge is  $r_e = h/3\lambda$ , where  $h$  is the height of the reflecting strip. The reflection coefficient per strip is therefore  $\sim 2h/3\lambda$ . Since the devices described

can accommodate up to  $\sim 360$  reflectors per transducer, a reflection coefficient approaching unity would obtain for an  $A\lambda$  thickness of  $\sim 300$  Å. Our normal device thickness is  $\sim 700$  Å, which allows for some reduction in reflection coefficient due to over-etching in fabrication. However, designs 4 and 6 of Table 1 were included to enable measurements to be made on devices with about half the number of unidirectional reflecting strips mentioned above. It should also be recalled from section 4 that we always have the option of reducing the number of rungs and reflectors in each transducer by laser burning. This process would not materially affect the spurious passband level in the devices used here.

Two batches of devices have been made and measured; these employed  $A\lambda$  thicknesses of 700 Å and 1500 Å. Various measurements were made on these devices and a number of useful conclusions drawn as discussed below:

(i) Results on Patterns 1 and 2 from Table 1

These measurements basically establish the properties of conventional SAW devices. Figure 19(a) shows the response of pattern 1 on ST-quartz untuned, the  $A\lambda$  thickness being 700 Å. A strong distortion is evident at the centre of the response, and is caused by reflections from the IDT fingers<sup>(23)</sup>. We may note that each transducer contains  $\sim 108$  finger pairs with  $\sim 225$  fingers of identical width and spacing to those we use in the unidirectional reflector banks. The significant reflection level indicated in Figure 19(a) may therefore be regarded as qualitative confirmation of our earlier estimates of the reflection coefficient levels. In Figure 19(b) we show the corresponding response of an untuned device of pattern 2, Table 1, which incorporate blooming, and is illustrated in Figures 19(d) and (e). This blooming has evidently removed the predominant source of spurious reflections in pattern 1, and has also produced a minor downshift in the centre frequency. Devices of this kind have long been used in RSRE as the feedback elements of SAW oscillators. In Figure 19(c) the transducers of this bloomed device have been tuned and matched to  $50 \Omega$  by means of shunt and series inductors. The loss is thereby reduced to 9 dB, but the response is evidently distorted by the triple-transit reflection; the three 'bumps' visible in the response are consistent with the triple-transit delay, the transducers being in close proximity, Figure 19(e). This measured loss of 9 dB basically comprises 6 dB bidirectionality loss and 3 dB miscellaneous loss (eg due to electrical finger resistance, bulk wave generation, acoustic loss and diffraction etc). However in this device the triple transit signal marginally reduces the loss at the centre frequency. It is the object of the group-type SPUDT investigation to reduce this loss further, and to produce a smoother passband.

(ii) Results on Patterns 3 and 4 of Table 1

These devices were tuned and matched much as devices 1 and 2 in the previous section. Each pattern produced a clean response with minimal inband ripple, and a reduced loss. In the case of pattern 3 the loss shown in Figure 20(a) is 6.7 dB, but other devices have shown losses as low as 6.0 dB. The expanded view of Figure 20(b) also shows a minimal deviation from linear phase.

Pattern 4 shows a marginally higher loss, Figures 20(d) and (e), and an even more linear phase response.

(iii) Results on Patterns 5 and 6 of Table 1

These designs were aimed to combine in each reflector bank the blooming and unidirectional reflector arrays. The effective number of unidirectional strips per transducer was  $\sim 280$  in pattern 5 and  $\sim 180$  in pattern 6, and so should have produced results comparable to patterns 3 and 4. Unfortunately they did not perform as expected, and at present the author has no satisfactory explanation of this behaviour. The responses of the devices (tuned and matched in a similar manner to the previous devices) are shown in Figure 21 for completeness.

### 5.3 MEASUREMENTS ON DEVICES EMPLOYING 1500 Å AL

Overall, the results were similar to those using 700 Å, but pattern 3 presumably possessed too strong a mass-loaded reflection level, Figure 22(a), while pattern 4, having fewer reflectors, behaved relatively well, Figure 22(b).

## 6 GROUP-TYPE SPUDT DEVICES ON AT-QUARTZ

This orientation of quartz is of interest as it has 2 marginal advantages over the ST-cut. Firstly, it has a slightly higher coupling constant,  $k^2$ , which can lead to a lower insertion loss in some circumstances, and, secondly, it has a higher turnover temperature, such that when partially metallised with the transducer structure its temperature coefficient of frequency (or delay) goes to zero at room temperature. A batch of devices has therefore been produced on this cut, the metal thickness being 900 Å. The behaviour of these devices is similar to the ST-cut, but with marginally lower loss, and a slightly lower frequency of operation due to the lower SAW velocity. Measurements on patterns 3 and 4 are shown in Figure 23, and represent our best group-type SPUDT results on quartz to date. At least part of the remaining  $\sim 6$  dB loss appears to come from a large background resistance in the transducers, evident in their  $S_{11}$  measurements. Relative to the SAW radiation resistance this loss is appreciably greater than the electrical finger resistance term expected for the AL thickness employed. One possible origin of this loss is an effective reduction in the piezoelectric coupling constant which occurs if there is an appreciable propagation loss between the rungs of a ladder transducer. Such an effect has been observed before in conventional SAW devices at high frequencies.

## 7 CONCLUSION

The objective of this work was to establish the viability of the group-type SPUDT structure as a means of realising high-fidelity low-loss SAW devices. The work described in the previous sections has, we believe, demonstrated this for both  $\text{LiNbO}_3$  and quartz, the two most commonly used SAW substrates. We therefore feel that the SPUDT approach can be considered for a number of applications, although at present it is still limited to narrow band responses. The impulse response model of Appendix 2 gives a good first-order account of the response (amplitude and phase) and, as in the case of the conventional SAW IDT, provides a good intuitive feel for the device behaviour. A more accurate approach is the COM (coupling of modes) analysis of Refs (12) and (13), but

the discerning reader may note a difference in design philosophy between the RFM workers and ourselves. RFM are principally concerned to minimise the triple transit signal and the concomitant passband distortion; our own primary goal has been to minimise the insertion loss, this being the parameter of paramount importance in certain front-end filter applications of which we are aware. This difference of approach is not fundamental; it merely reflects the different specifications encountered by the two groups to date.

During the course of this Memorandum various suggestions have been made of ways to improve further the range and/or performance of such SPUDT devices. In particular it is hoped that others will extend this study to cover other substrates, waves, reflection mechanisms, and SPUDT transducer structures.

#### REFERENCES

- 1 H Matthews (ed), 'Surface Wave Filters' (Wiley, 1977).
- 2 M F Lewis, C L West, J M Deacon and R F Humphryes, 'Recent developments in SAW devices', IEE Proceedings part A (1984) pp 186-215.
- 3 F G Marshall, E G S Paige and A S Young, 'New Unidirectional Transducer and Broadband Reflector of SAW', Electronics Letters 7 (1971) pp 312-314.
- 4 R C Rosenfeld, C S Hartmann and R B Brown, 'Low-loss Unidirectional SAW Filters', Proc. 28th Annual Frequency Control Symposium, pp 299-303.
- 5 E A Ash, 'Surface wave grating reflectors and resonators', IEEE Symposium on Microwave Theory and Techniques, Newport Beach, May 1970.
- 6 E J Staples, J S Schoenwald, R C Rosenfeld and C S Hartmann, 'UHF surface acoustic wave resonators', Proc. 1974 IEEE Ultrasonics Symposium, pp 245-252.
- 7 F G Marshall, 'SAW resonators constructed of Al<sub>2</sub>O<sub>3</sub> on ST-quartz for use in high stability feedback oscillators', Proc. 1975 IEEE Ultrasonics Symposium, pp 290-292.
- 8 M F Lewis, 'SAW filters employing interdigitated interdigital transducers', Proc. 1982 IEEE Ultrasonics Symposium, pp 12-17.
- 9 F Sandy and T E Parker, 'SAW ring filter', Proceedings 30th Annual Frequency Control Symposium 1976, pp 334-339.
- 10 Y Kinoshita, M Hikita, T Tabuchi and H Kojima, 'Broadband resonant filter using surface-shear-wave mode and twin-turn reflector', Electronics Letters 15 (1979) pp 130-131.
- 11 D J Gunton, M F Lewis and E G S Paige, 'The travelling wave transducer', Proc. 1975 IEEE Ultrasonics Symposium, pp 422-5.
- 12 C S Hartmann, P B Wright, R J Kansy and E M Garber, 'An analysis of SAW IDTs with internal reflections and the application of the design to single-phase unidirectional transducers', Proceedings of the 1982 IEEE Ultrasonics Symposium, pp 40-45.

- 13 P V Wright and S A Wilkins, 'A prototype Low-Loss Filter employing single-phase unidirectional transducers', Proc. 1983 IEEE Ultrasonics Symposium, pp 72-6.
- 14 R H Tancrell and M G Holland, 'Acoustic surface wave filters', Proc. IEEE 59 (1971), pp 393-409.
- 15 F A Jenkins and H E White, 'Fundamentals of optics' (McGraw-Hill, 1957).
- 16 D M Kerns and R W Beatty, 'Basic theory of waveguide junctions and introductory microwave network analysis' (Pergamon Press, 1967).
- 17 W R Smith, H M Gerard, J H Collins, T M Reeder and H J Shaw, 'Design of surface wave delay lines with interdigital transducers', IEEE Trans MTT-17, 1969, pp 865-873.
- 18 M F Lewis, 'A different approach to the wave scattering properties of interdigital transducers', IEEE Trans SU-30 (1983) pp 55-57.
- 19 M F Lewis, 'Low-loss SAW Devices employing Single Stage Fabrication', Proc. 1983 IEEE Ultrasonics Symposium, pp 104-108.
- 20 C Dunnrowicz, F Sandy and T Parker, 'Reflection of SAW from Periodic Discontinuities', Proc. 1976 IEEE Ultrasonics Symposium, pp 386-390.
- 21 E G S Paige, A G Stove and R C Woods, 'SAW reflection from aluminium strips on LiNbO<sub>3</sub>', Proc. 1981 IEEE Ultrasonics Symposium, pp 144-7.
- 22 M F Lewis, 'The surface acoustic wave oscillator - a natural and timely development of the quartz crystal oscillator' Proceedings of the 28th Annual Frequency Control Symposium, 1974, pp 304-314.
- 23 W S Jones, C S Hartmann and T D Sturdivant, 'Second order effects in surface wave devices', IEEE Trans SU-19 (1972) pp 368-377.

## APPENDIX 1

In the text it is suggested that the development of compact low-loss SAW bandpass filters can be exploited by cascading such devices to provide entirely passive filters with extreme out-of-band rejection, and still having an insertion loss considerably lower than conventional SAW bandpass filters. At the time of writing this Memorandum the author did not have available a suitable number of SPUDT devices, so the tests were conducted on similar low-loss devices employing the IIDT structure<sup>(8)</sup>. The first step was to demonstrate that 4 devices in series had the bandpass characteristics expected from elementary considerations, eg four times the loss, and a bandshape scaled by a factor of four on a dB scale. That this is approximately true is illustrated in Figure A1 by plotting the response of one device at 5 dB/div, and the response of the 4 devices at 20 dB/div. Note that it is not obvious that such a result obtains exactly, since the ports of the individual devices are not all perfectly matched to 50  $\Omega$ . Indeed there would appear to be scope for improving the out-of-band rejection in such a scheme by simply mismatching the impedances of the cascaded ports at frequencies out-of-band. Nevertheless the result of Figure A1 is, to first order, as expected from elementary considerations. It demonstrates that an acceptable loss ( $\sim 8$  dB) and high rejection are possible in such cascaded devices. Of course the demonstration provided in Figure A1 is about the worst case imaginable, as all four responses are virtually identical (such is the reproducibility of SAW devices!) so that all the spurious signals add coherently, enhancing the in-band ripple, and the out-of-band rejection minima. As a trivial demonstration that improvements are possible in these respects the author has heated two of the devices by  $\sim 100^\circ\text{C}$  by the application of soldering irons to their PCBs (such is the robustness of SAW devices!). The large temperature-coefficient of frequency of YZ-LiNbO<sub>3</sub> ( $\sim -100$  ppm/ $^\circ\text{C}$ ) causes a sufficient relative frequency shift to smooth out much of the ripple, resulting in an impressive filter characteristic, Figure A2. It will be self-evident to the reader that a serious design effort could not fail to produce even more impressive results, with losses  $\sim 10$  dB and rejection  $\geq 90$  dB. These filters could be fabricated on a single chip, and the preferred arrangement is transversal, to avoid spurious wave coupling effects in a longitudinal array. This approach could well herald in a new era in high-performance SAW bandpass filter technology.

## APPENDIX 2

The  $\delta$ -function model of a SAW interdigital transducer was mentioned briefly in section 2, and leads to a ready appreciation and visualisation of the operation of and frequency response of conventional SAW devices. Indeed the author would argue that the extreme simplicity and considerable accuracy of this approach at the fundamental frequency have been prime factors in the successful exploitation of SAW devices in commercial markets. It is therefore of interest to extend this approach to the SPUDT devices described in this Memorandum in order to gain insight into their operation. It should be emphasised that such an approach is only valid in the limit of weak reflections. Strictly one should include multiple reflections in such an analysis. However, if this were attempted the computation time would diverge, and alternative approaches such as the COM approach<sup>(12,13)</sup> would be the only practicable solution. We have therefore pursued the  $\delta$ -function approach in its simplest form, but have included checks on its validity at various points in the work.

The principle is best illustrated by example. Let us analyse the especially simple SPUDT transducer illustrated in Figure A3(a), comprising a small number of  $\delta$ -function rungs,  $N = 6$ . Between these rungs and slightly offset ( $\lambda/8$ ) are 5  $\delta$ -function reflectors. If this transducer is impulsed and monitored by a simple output transducer to its left or right (as illustrated) its output in the limit of weak reflections will contain 6 strong impulses corresponding to the 6 rungs, and collectively constituting the impulse response,  $h_0(t)$ , of the ladder transducer alone. In addition the full impulse response,  $h(t)$  will contain the sets of reflected impulses shown in Figure A3(b).

If for simplicity we imagine that the reflections arise from the impedance discontinuity of the reflecting strips, and consider only the reflections from the edges which coincide with the physical centres of the rung-rung period, Figure A3(a), it will be evident that the reflection coefficients are opposite in sign for the two directions, Figure A3(b). The net impulse responses are as shown in Figure A3(c), and the Fourier Transforms of these give the net frequency responses in the forward and reverse directions as shown schematically to the right of the impulse responses in Figure A3. This basic procedure led to the calculated frequency responses of Figures 7-10.

The general form of the net amplitude and phase plots in Figures 7-10 may be verified qualitatively by the following considerations. Firstly note that for large  $N$ , the contribution of the reflections to the impulse response,  $h_r(t)$ , comprises a periodic impulse train under a diamond-shape envelope of twice the duration of  $h_0(t)$ . This envelope may be regarded as the convolution of two rectangular envelopes, each being of the same duration as  $h_0(t)$ . If the frequency response of  $h_0(t)$  is written  $\text{sinc}(x)$ , then the convolution theorem assures us that the frequency response of  $h_r(t)$  has modulus  $\text{sinc}^2(x)$ , ie its main lobe has the same width as  $H_0(f)$  but is more sharply peaked at the centre frequency. Further, the centre of  $h_r(t)$  is displaced from the centre of  $h_0(t)$  by  $\sim (N/2)$  periods at  $f_0$ . Thus while  $h_0(t)$  and  $h_r(t)$  are exactly in or out of phase at  $f_0$ , this phase relationship changes away from the centre frequency leading to destructive interference at the edges of the forward response, and constructive interference at the edges of the reverse response. This behaviour, and also the phase deviations of the resultant are best visualised by means of phasor diagrams as in the case of optical interference (Ref (15), Figure 17H).

## LOW LOSS SAW DEVICES EMPLOYING SINGLE STAGE FABRICATION

Meirion Lewis

Royal Signals and Radar Establishment,  
Malvern, Worcestershire, United Kingdom.

## Abstract

This paper describes a development of the SPUOT (single phase unidirectional transducer) concept. The new design employs 'sampled' transducers to allow the introduction of reflector banks within the transducers. The fabrication of such devices requires a single stage of photolithography. Prototype devices have shown very encouraging passband characteristics with an insertion loss of less than 3 dB on  $\text{LiNbO}_3$ .

## 1. Introduction

In the past numerous designs of surface acoustic wave (SAW) bandpass filters have been reported based on a variety of interdigital transducer (IDT) geometries<sup>(1)</sup>. Such devices offer the systems engineer a number of attractive features: SAW filters are small, cheap, rugged, reproducible, passive, planar components covering the range from 10 MHz to > 1 GHz and displaying excellent group delay and stop band rejection characteristics. Most such filters incur an insertion loss of order 20 dB, since by accepting this loss the design procedure is simplified and the effect of the spurious triple transit signal is made minimal. At i.f. such a loss is often acceptable as it does not degrade the signal/noise ratio significantly, and the loss itself is readily made good by means of an additional stage of i.f. amplification. It is, however, self-evident that filters with a lower loss are preferable, and in some applications they are vital (eg for front-end filtering, and in applications demanding minimum size and power consumption). To this end SAW research workers have devised several techniques for reducing the loss of SAW filters to a few dBs. These include multistrip coupler-based unidirectional IDT's<sup>(2)</sup>, multiphase IDT's<sup>(3)</sup>, two-port resonators<sup>(4)</sup>, interdigitated IDT's<sup>(5)</sup> and a family of 'ring' filter arrangements<sup>(6,7)</sup>. Most of these devices incur one or more penalties, eg increased substrate area, more complex fabrication and matching circuitry, and/or a restricted range of realizable filter characteristics. A recent addition to this list of low-loss filter techniques is the structure of Hartmann et al<sup>(8)</sup> which reduces the 3 dB bidirectionality loss of each IDT by incorporating an (offset) reflector array to enhance the required forward wave at the expense of the unwanted backward wave. The experimental arrangement used by Hartmann et al to demonstrate the principle comprised an array of gold reflectors deposited on to the aluminium IDT's in a second metal evaporation process.

In this letter we describe a novel arrangement whereby the reflector bank is generated in the same photolithographic process (and from the same metal) as the IDT itself, thereby simplifying the fabrication, and relieving the problem of alignment between the reflectors and IDT's. Prototype devices have demonstrated an insertion loss of less than 3 dB on  $\text{LiNbO}_3$ .

## 2. Description of New Device

The basic arrangement is shown schematically in Fig 1 and comprises two 'ladder' transducers with (offset) reflector banks in the spaces between the active 'rungs' of each ladder. Such ladder IDT's have been used in the past in a variety of applications. The attraction of Fig 1 is immediately apparent - the reflector array is fabricated in the same photolithographic process as the transducers, and the unidirectional transducers occupy a space only marginally (if any, see discussion) greater than their bidirectional counterparts.

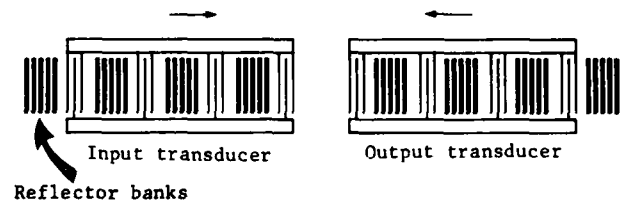


Figure 1. Schematic of unidirectional-transducer SAW device employing offset reflector banks. As discussed in the text the designs of the two IDT's will normally be different to avoid spurious passbands caused by the 'sampling' process.

## 3. Operation of New Device

Hartmann et al<sup>(8)</sup> have used a coupling-of-modes theory to describe the operation of a conventional IDT with a superimposed reflector array. An important result to emerge from this theory is that the individual reflectors should be offset from the transducer fingers by  $\pm \lambda/8$  for optimum operation ( $\lambda$  = SAW wavelength at the centre frequency). We show below that a similar result obtains for the ladder transducer arrangement of Fig 1. In Fig 2 we show an expanded view of a section of one IDT, and for simplicity we replace the reflector bank by a single reflecting strip.

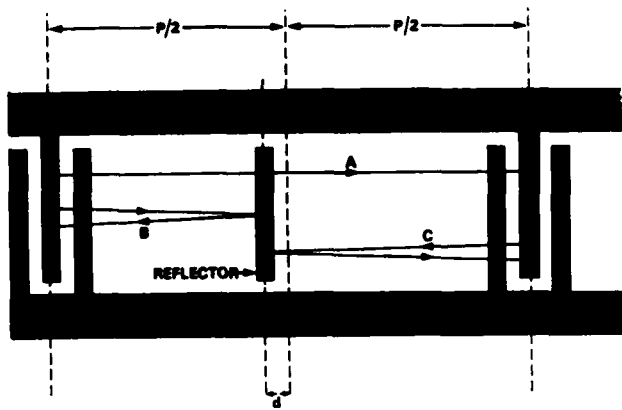


Figure 2. Schematic view of a section of one of the transducers of Fig 1.

At the centre frequency there must be constructive interference between the waves excited by each rung of the ladder IDT (waves A in Fig 2) so that

$$\frac{P}{\lambda} + \angle S_{12} = 2n\pi, n = \text{integer} \quad \dots (1)$$

here  $\frac{P}{\lambda}$  is the phase lag over one period,  $P$ , in the absence of the reflector, and the term  $\angle S_{12}$  in S-parameter notation accounts for the additional phase shift incurred in transmission when the reflector is present. Throughout this discussion we shall assume that the transducer rungs and reflector banks are symmetrical structures, and refer all phases to their centres. We shall initially ignore any reflections from the transducers themselves, a situation we approximate experimentally by the use of split-finger transducers. For constructive interference to the left, and destructive interference to the right, the reflected waves B and C must satisfy the additional conditions.

$$\text{wave B, } \frac{P}{\lambda} + \angle S_{11} - 2/d = 2n\pi \quad \dots (2)$$

$$\text{wave C, } \frac{P}{\lambda} + \angle S_{11} + 2/d = 2n\pi \pm \pi \quad \dots (3)$$

where  $\angle S_{11}$  is the phase shift on reflection, referred to the centre of the reflecting strip.

Equations (2) and (3) give  $4/d = \pm \pi$ , or

$$d = \pm \lambda/8 \quad \dots (4)$$

Equations (1) to (3) then lead to

$$\angle S_{11} - \angle S_{12} = \pm \frac{\pi}{2} \quad \dots (5)$$

The  $\pm$  signs must be used consistently in Eqns (4) and (5). Similarly it is readily shown that for unidirectional transduction to the right

$$\angle S_{11} - \angle S_{12} = \pm \frac{\pi}{2}, d = \mp \lambda/8 \quad \dots (6)$$

In the author's view it is not obvious that these conditions can be satisfied, but in Appendix 1 we show that providing the reflecting arrays constitute symmetrical reciprocal lossless 2-port

junctions, the conditions (5) or (6) are met on any substrate regardless of the detailed reflection mechanism(s).

This result is highly fortuitous for the operation of such unidirectional transducers. The only assumption in doubt above is that of losslessness. Fortunately we know from experiments on SAW resonators(4) that reflecting arrays can behave extremely well in this respect. In any case if the reflectors were lossy, they would not be of great use in unidirectional transducers, one of whose primary functions is to reduce the device insertion loss. On a given substrate, ie for a given sign of  $\angle S_{11} - \angle S_{12}$ , Eqns (5) and (6) show that the two transducers of a low-loss SAW device should employ opposite offsets of  $d = \pm \lambda/8$ , as indicated schematically in Fig 1.

#### 4. Experimental Results on LiNbO<sub>3</sub>

In order to test these principles a few simple test patterns have been produced and have indeed demonstrated low-loss operation on YZ-LiNbO<sub>3</sub> and 128° LiNbO<sub>3</sub>. The principal results are presented in Fig 3.

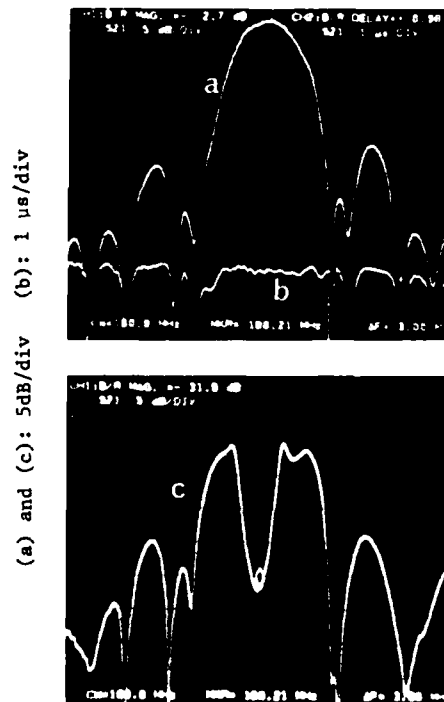


Figure 3. Experimental results on unidirectional SAW filter. (a) and (b) show the transmission ( $S_{12}$ ) and group delay of a device operating correctly with transducers face-to-face. Curve (c) shows the transmission characteristics of a device with transducers back-to-back.

The design details are as follows: the transducers employed split fingers of  $70 \lambda$  aperture and each comprised 10 'rungs' of two acoustic periods (two split fingers into 3 split fingers) per rung, ie 20 active periods per transducer. One transducer employed a rung-to-rung period  $P = 8 \lambda$  with 10 reflecting strips per bank, each reflector strip (and gap) being of width  $\lambda/4$ , where  $\lambda = 34.5 \mu\text{m}$ . The other transducer employed  $P = 10 \lambda$  with 14 reflecting strips per bank. As discussed later, by so staggering the designs the overall response contained just the one principal transmission peak shown in Fig 3(a). The fractions of the transducer metallized were made very similar to avoid a differential frequency shift through slowing of the SAW in the metallized sections<sup>(9)</sup>. For correct operation on YZ-LiNbO<sub>3</sub> the reflector banks in each transducer were off-set  $\lambda/8$  towards the other transducer. The YZ-LiNbO<sub>3</sub> chip is mounted in a TO8 container with gold wire bonds to the 1500Å-thick Al contact pads. A close match to 50 ohms was achieved by shunt-tuning each transducer with a wirewound inductor of c.100 nH. The resulting insertion loss of 2.7 dB at the fundamental frequency of 100 MHz confirms the unidirectionality of transduction, for a conventional SAW device with bidirectional transducers has a minimum theoretical loss of 6 dB (and in practice a matched loss of typically 8 to 10 dB). The high degree of unidirectionality is further illustrated by measurements on a device with the transducers back-to-back; this displays a loss of c.30 dB at the centre frequency, Fig 3(c). Two other features worthy of note in Fig 3 are the low levels of the passband ripple ( $< 0.5$  dB peak-to-peak) and of the group delay ripple ( $\pm 100$  ns, in band), each feature being important in certain applications. Further, if one is prepared to accept ripple in these latter parameters it is also interesting to note that the insertion loss of this particular filter is only 3.0 dB with the transducers untuned, another feature of significance in some applications, e.g. those demanding minimum size and/or cost and/or vibration sensitivity.

### 5. Discussion of results on LiNbO<sub>3</sub>

In section 4 we described a device with a high degree of unidirectionality resulting in an insertion loss of  $< 3$  dB. Similar results have been obtained for the same device pattern on 128° LiNbO<sub>3</sub>. This high degree of unidirectionality is expected for the device described in section 4 because the transducers contain a total of 100 and 140 reflecting strips respectively, and each strip has an amplitude reflection coefficient of order 1%<sup>(10,11)</sup>. The work of Paige et al<sup>(10)</sup> shows that the device of Fig 3 undoubtedly employs piezoelectric shorting as the principal reflection mechanism. This is confirmed by the weak reverse unidirectionality of the transducers operated at their 3rd harmonic response (300 MHz). At this frequency the reflectors have a width  $\sim 0.75 \lambda'$  and an offset  $3 \lambda'/8$ , where  $\lambda'$  is the SAW wavelength at 300 MHz. The unidirectionality is expected to be weak in these circumstances as the reflection coefficient approaches zero for this particular reflector width (ref 10, Fig 3), and is

expected to be reverse because in reflection an offset of  $3 \lambda'/8$  is equivalent to an offset of  $-\lambda'/8$ . In one device we have experimentally increased the degree of unidirectionality at the 3rd harmonic by overetching in fabrication to reduce the reflector widths to  $\sim 0.6 \lambda'$ . Again this is consistent with ref 10 Fig 3 which shows a peak reflection coefficient for a width of about  $0.5 \lambda'$ ; such a structure could be useful to implement high frequency unidirectional SAW devices.

Another design option at our disposal on strong piezoelectrics (but absent from the device of ref (8)) is the ability to modify the reflection coefficient by electrically shorting the reflector banks to form "grid-iron" structures. We have performed this test on a YZ-LiNbO<sub>3</sub> device which is otherwise of the design described in section 4, and have observed that the sense of unidirectionality is thereby reversed. This observation is consistent with the results of Dunnrowicz et al, ref 11, table 1.

### 6. Conclusion and Discussion

We have described a new arrangement of transducers and reflectors which can be fabricated in a single photolithographic process, and which achieves a high degree of unidirectionality. In the limit of one rung and one reflector bank per transducer this device degenerates into a two-port resonator. It is too early to give a realistic assessment of all the advantages and disadvantages of this new arrangement relative to the other low loss techniques<sup>(2-8)</sup>, but as pointed out by Hartmann et al<sup>(8)</sup>, the use of multiple reflectors provides a great design flexibility, for example in the device in Fig 1 each reflector bank (as well as the active 'rungs') can be weighted in a variety of ways (e.g. number, position, width, length) to achieve the required overall bandpass characteristics. Even so, the initial unweighted test device of Fig 3 displays many encouraging features, viz low-loss, low in-band transmission ripple, low group delay ripple, and of course simple fabrication.

Concerning the frequency response of a generalized (weighted) version of the device illustrated in Fig 1 we may make the following remarks. Firstly, we recall that a single conventional SAW transducer is, in principle, capable of yielding an arbitrary bandpass response with substantially independent phase and amplitude characteristics, apart from a constant group delay<sup>(1)</sup>. A real device comprises two transducers and the overall response may be divided between these in a variety of ways; the response achieved in practice is limited by the finite size of the acoustic substrate. Ignoring the reflectors for the moment, the ladder transducers of Fig 1 may be regarded as sampled versions of a conventional IDT. We may then invoke the Nyquist sampling theorem to show that providing the sampling period (time)  $\leq 1/2B$  where  $B$  is the width of the required (band-limited) response, the consequence of the sampling is merely to introduce spurious passbands at intervals equal to the reciprocal of the sampling period. If we then choose the sampling period of

the second transducer so that the spurious pass-bands do not overlap, we essentially reproduce the bandpass characteristics of the unsampled transducers. The device of Fig 3 is an example of this concept. This suggests that the sampling procedure (which is, of course, necessary in order to introduce the 'printed' reflectors into the device of Fig 1) will not significantly degrade the design-flexibility of SAW devices. In any case it should be noted that sampled (ie. ladder) transducers are already employed in various SAW devices. In the limit of weak reflections, similar arguments apply to the frequency response of the (sampled) reflector arrays, except that the unidirectionality is narrower-band due to the multiplicity of double-transits involved. This feature is evident on comparing figs 3(a) and 3(c), and suggests that (depending on the band-shape required) a useful design procedure might be to concentrate the reflectors in the centre of each transducer.

The discussion so far has centred around the specific test pattern on  $\text{YZ-LiNbO}_3$  described in section 4. It is clear, however, that numerous variations in the details are possible, and should permit the development of a wide range of devices for different applications. For example, the transducer sections may employ conventional IDT's, split-finger IDT's, "2 into 1" IDT's<sup>(14)</sup>, bloomed IDT's<sup>(15)</sup>, etc and may be weighted in a variety of ways, e.g. apodized, phase-weighted, withdrawal-weighted ... . The reflector banks may comprise isolated metal strips, shorted strips, earthed strips, various weighted arrays, or even grooves, but this latter option would detract from the fabrication simplicity. An advantage over the original SPUDT arrangement<sup>(8)</sup> is the ability of the arrangement of Fig 1 to exploit reflections from mass-loading, topography, piezoelectric shorting, regeneration, or any desired combination of effects. The waves employed may be SAW, pseudo-SAW, BG-waves, SSBW etc, and the substrate may be any piezoelectric, or a non-piezoelectric substrate with piezoelectric overlay. An obvious candidate is SAW on ST-quartz for the temperature-stable operation of relatively narrow-band devices, e.g. for oscillator control<sup>(15)</sup>. On this material we have produced similar results to the original SPUDT (ref 8, Fig 7a) using the new arrangement of Fig 1. The principal difference from the design of the  $\text{LiNbO}_3$  device of section 4 is the necessity to offset the reflectors away from the other transducer on ST-quartz. This result is consistent with refs (4) and (11).

#### Acknowledgement

The author gratefully acknowledges the assistance of George Gibbons and David Snell in producing the masks for the new transducers described here.

Copyright © Controller, HMSO, 1983.

#### References

1. H. Matthews. (Ed) 'Surface Wave Filters' (Wiley, 1977).
2. F.G. Marshall, E.G.S. Paige, and A.S. Young. 'New Unidirectional Transducer and Broadband Reflector of SAW' Electronics Letters 1971, 7 pp 312-314.
3. R.C. Rosenfeld, C.S. Hartmann and R.B. Brown. 'Low-loss Unidirectional SAW Filters' Proc. 28th Annual Frequency Control Symposium pp 299-303.
4. F.G. Marshall, 'SAW resonators constructed of Al on ST-quartz for use in high stability feedback oscillators' Proc. 1975 IEEE Ultrasonics Symposium pp 290-292.
5. M.F. Lewis, 'SAW filters employing interdigitated interdigital transducers' Proc 1982 IEEE Ultrasonics Symposium pp 12-17.
6. F. Sandy and T.E. Parker, 'SAW ring filter' Proceedings 30th Annual Frequency Control Symposium 1976, pp 334-339.
7. Y. Kinoshita, M. Hikita, T. Tabuchi and H. Kojima, 'Broadband resonant filter using surface-shear-wave mode and twin-turn reflector' Electronics Letters 1979, 15, pp 130-131.
8. C.S. Hartmann, P.B. Wright, R.J. Kansy and E.M. Garber, 'An analysis of SAW IDT's with internal reflections and the application of the design to single-phase unidirectional transducers' Proceedings of the 1982 IEEE Ultrasonics Symposium, pp 40-45.
9. R.S. Wagers, 'Phase error compensation in finger withdrawal transducers', Proceedings 1974 IEEE Ultrasonics Symposium, pp 418-421.
10. E.G.S. Paige, A.G. Stove and R.C. Woods, 'SAW reflection from aluminium strips on  $\text{LiNbO}_3$ ' Proceedings 1981 IEEE Ultrasonics Symposium, pp 144-147.
11. C. Dunnrowicz, F. Sandy and T. Parker, 'Reflection of SAW from Periodic Discontinuities' Proc 1976 IEEE Ultrasonics Symposium pp 386-390.
12. R.L. Rosenberg, 'Wave-scattering properties of interdigital SAW transducers' IEEE Trans SU-28 (1981) pp 26-41.
13. M.F. Lewis, 'A different approach to the wave-scattering properties of interdigital transducers' IEEE Trans SU-30 (1983) pp 55-57.
14. S.J. Kerbel, 'Design of harmonic SAW oscillators' Proc 1974 IEEE Ultrasonics Symposium pp 276-281.
15. M.F. Lewis, 'The SAW Oscillator - a natural and timely development of the quartz crystal oscillator' Proc 28th Annual Frequency Control Symposium (1974) pp 304-314.

Appendix 1

In section 3 we showed that devices of the structure of Fig 1 would possess unidirectional properties if Eqns (5) or (6) were satisfied. In this appendix we show on general grounds that this is so, providing that the reflector banks behave as symmetrical reciprocal lossless 2-port junctions. A mathematical derivation of the result has been given by Rosenberg, Ref 12, App III. Here we provide a more physical derivation - we note that a reflector bank comprising a symmetric (eg periodic) array of reflectors constitutes a reciprocal symmetrical 2-port junction. If we add the plausible assumption that this junction is also lossless, we can show that the transmitted and reflected amplitudes  $S_{12}$  and  $S_{11}$  (arising from a wave of unit amplitude incident from one side, viz port 1) are in phase quadrature when referred to the centre of the reflector bank. This result can readily be obtained by a minor modification of a recent publication by the author on the corresponding 3-port problem<sup>(13)</sup>. In the spirit of the latter approach the wave of unit amplitude incident on the reflector bank from one side (port 1) is transformed into symmetric and antisymmetric combinations of waves incident from both sides (ports 1 and 2), viz  $\begin{pmatrix} 1 \\ 0 \end{pmatrix} = \begin{pmatrix} +\frac{1}{2} \\ +\frac{1}{2} \end{pmatrix} + \begin{pmatrix} +\frac{1}{2} \\ -\frac{1}{2} \end{pmatrix}$ , Fig A1.

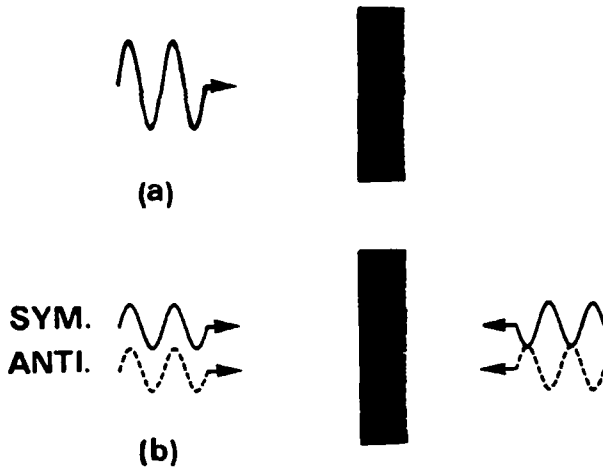


Figure A1 Illustrating the transformation of an incident wave into symmetric and antisymmetric pairs of equal amplitude.

These particular (orthogonal) combinations are chosen because they are not mutually coupled by a symmetric (or antisymmetric) junction, and so each emerges at full intensity but, in general, with a phase-shift, ie they emerge as  $\begin{pmatrix} +A \\ +A \end{pmatrix}$  and  $\begin{pmatrix} +B \\ -B \end{pmatrix}$  with  $|A| = |B| = \frac{1}{2}$ . Thus  $S_{11} = (A + B)$  and  $S_{12} = (A - B)$  are orthogonal, since the scalar product of  $(A + B)$  and  $(A - B)$  vanishes if  $|A| = |B|$ . This is illustrated in Fig A2.

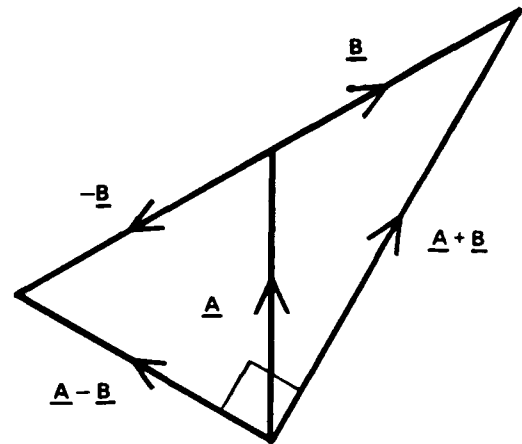


Figure A2. Geometrical construction showing that  $|A| + |B|$  and  $|A| - |B|$  are orthogonal if  $|A| = |B|$

In addition to this phase shift of  $\pi/2$  between the transmitted and reflected waves, it is apparent from Fig 2 that by offsetting the centre of the reflector bank from the centre of the rungs by  $\pm \lambda/8$ , the reflected waves B and C suffer additional phase shifts of  $\pm \pi/2$  relative to the transmitted waves, A. As a consequence of these combined phase shifts there is perfectly constructive interference in one direction and destructive interference in the other. However, from these arguments alone we cannot say which is the constructive direction, and indeed it may differ for the same device pattern on different piezoelectrics e.g. due to the differing nature of the reflection mechanism. It is therefore best found by experiment. It should be emphasized that the basic conclusion concerning the optimum offset of  $\pm \lambda/8$  is independent of the nature of the reflection mechanism, for example, in SAW devices it obtains for reflections arising from mass-loading, topographical effects, piezoelectric shorting or any combination thereof, providing only that the reflectors are essentially lossless. The experimental results of ref (11) are consistent with this conclusion. It is also interesting to note that according to these arguments a judicious choice of substrate and reflector strip parameters can result in constructive or destructive interference between the individual reflection mechanisms. Thus by choosing the piezoelectric substrate, and the material and geometry of the strip correctly, one should be able to enhance the reflections, e.g. for use in the present device, or cancel reflections to reduce undesirable effects in more conventional SAW devices, a possibility first mooted by Marshall<sup>(4)</sup>. In this context another variable at one's disposal is the ability to electrically short circuit the reflectors in each bank, as this can modify or even reverse the reflection coefficient, as discussed in the text.

The effect of losses can be seen qualitatively

from Fig A2. If the symmetric and antisymmetric pairs suffer equal losses, the conclusions are unaffected. It is typical of such systems, however, that the losses of these pairs will be unequal (e.g. because only one induces currents in the metallic strips). In general this will perturb the quadrature phase relationship derived above. Fortunately the SAW losses in reflector banks are known to be extremely small, so it is unlikely that any significant departures will arise from the optimum design procedure described in the text.

acoustic  
aperture

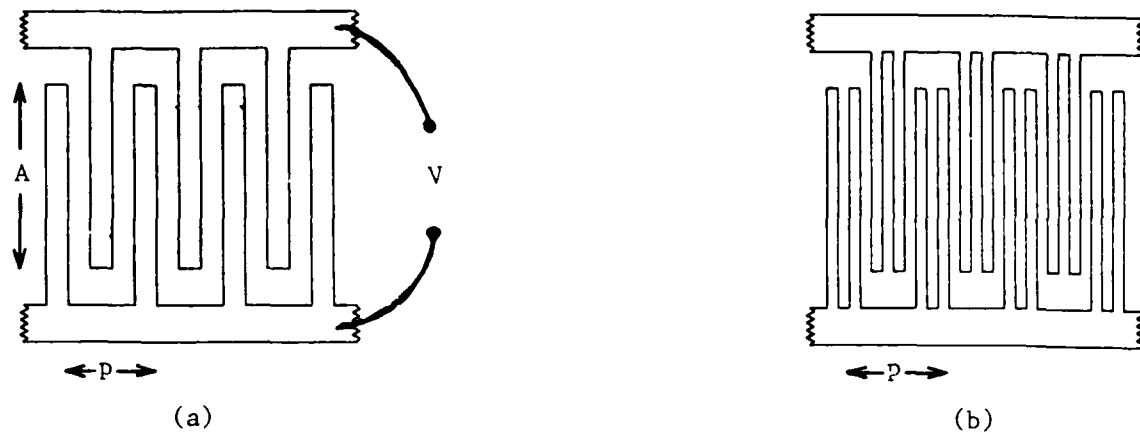


Figure 1. (a) Schematic of a conventional interdigital transducer of period,  $p$ , and aperture,  $A$ . (b) A similar device employing split-fingers.

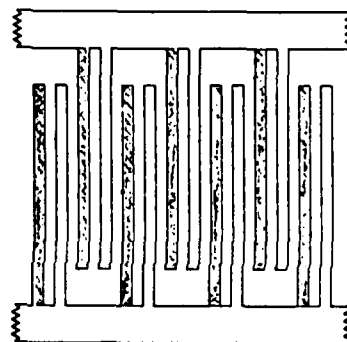


Figure 2. A schematic view of the original SPUDT device employing an antisymmetric array of gold reflectors (shaded) deposited on top of the symmetric  $A\lambda$  split-finger transducer.

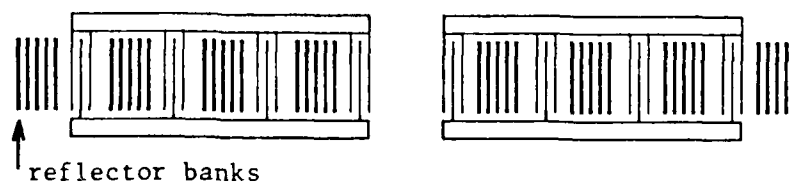


Figure 3. Schematic of a unidirectional SAW device employing offset reflector banks. As discussed in the text the design of the individual transducers will normally be different to avoid spurious passbands caused by the 'Sampling' process.

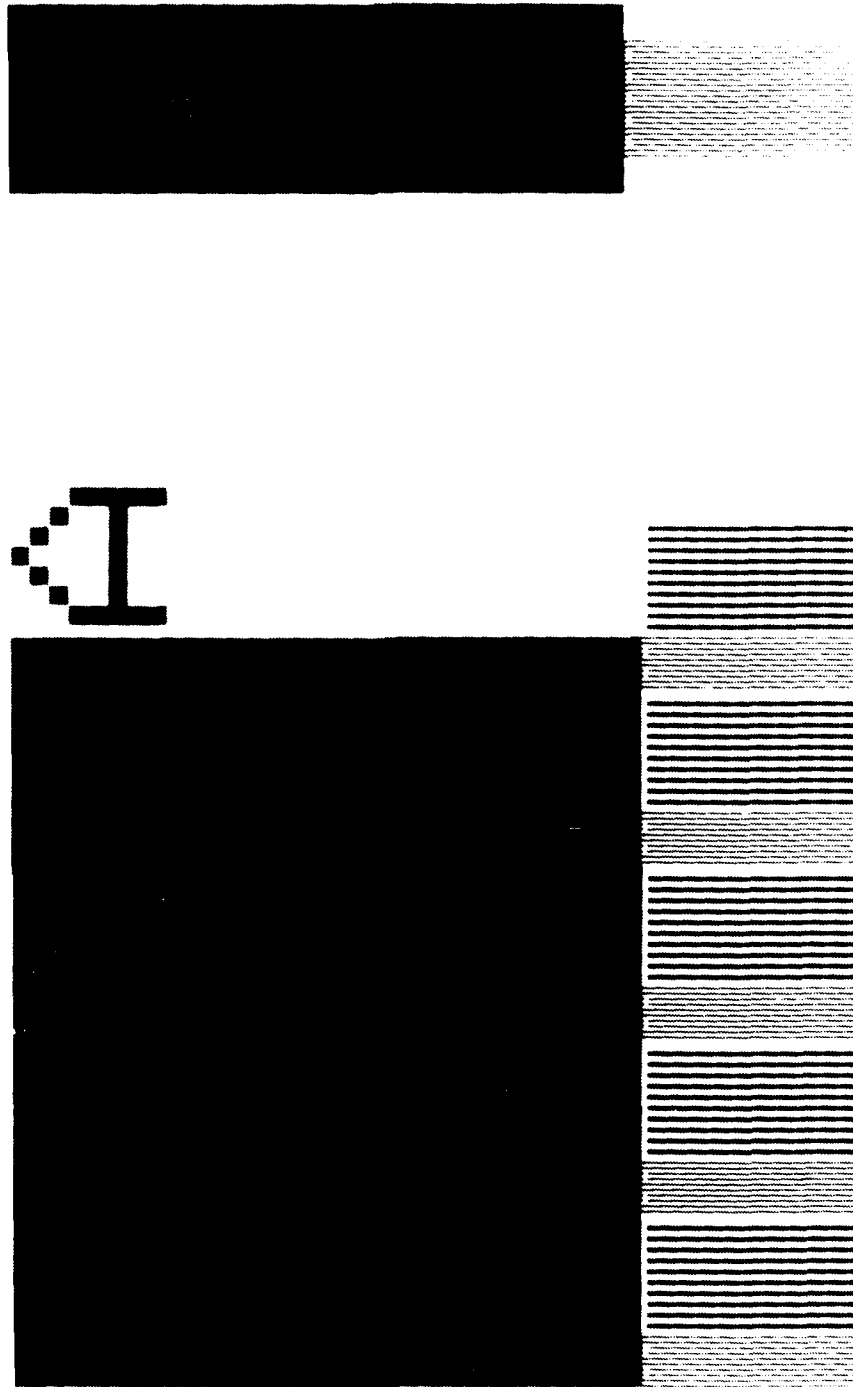
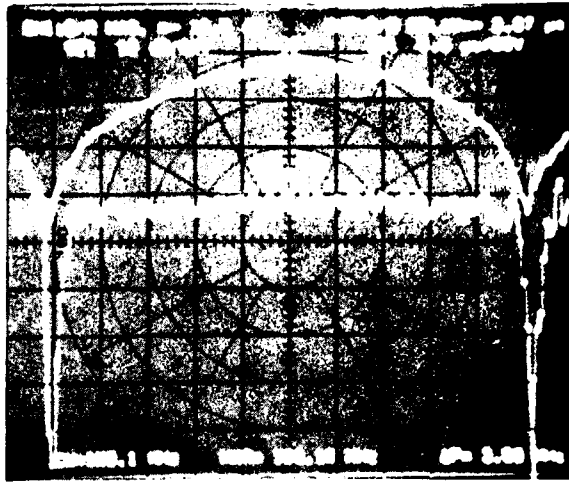


Figure 4. Photographs of parts of the SPUDT test pattern AW1724, viz transducer 'A' and one of the surrounding monitoring split-finger transducers.

S<sub>12</sub>  
10 dB/div

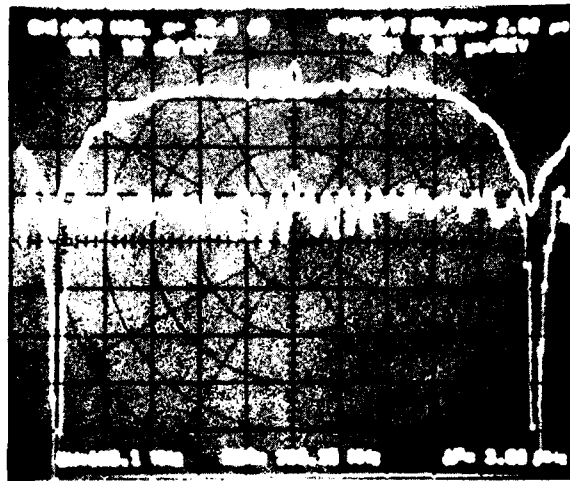
DELAY  
0.5 μs/div



(a)

S<sub>12</sub>  
10 dB/div

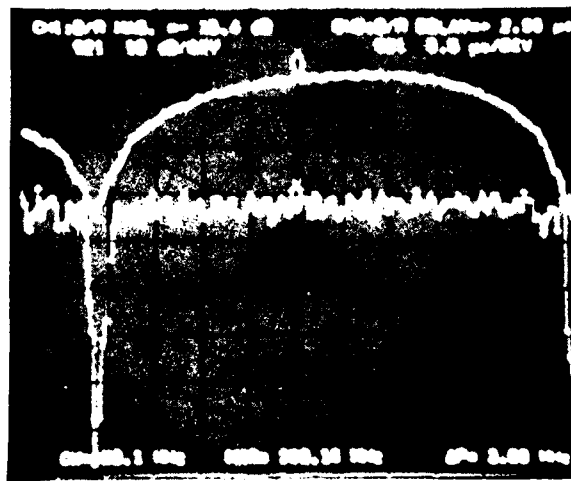
DELAY  
0.5 μs/div



(b)

S<sub>12</sub>  
10 dB/div

DELAY  
0.5 μs/div



(c)

CENTRE FREQUENCY, 100 MHz. 0.5 MHz/div

MEASURED TRANSMISSION AND GROUP DELAY CHARACTERISTICS OF UNTUNED GROUP-TYPE SPUDT TEST PATTERNS, (a) AND (b), COMPARED WITH LADDER TRANSDUCER WITHOUT REFLECTOR BANKS, (c).

(DEVICES A AND C, Bk 11E p36)

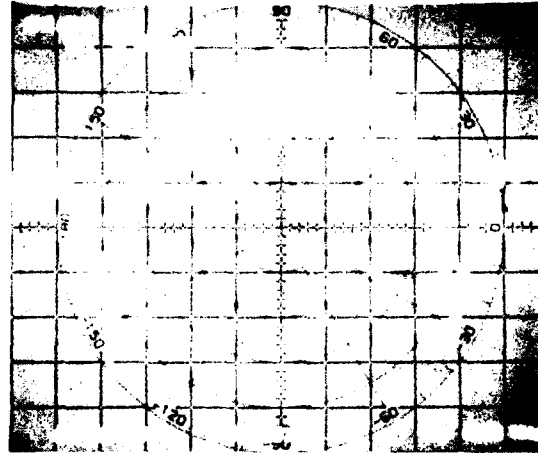
Figure 5

5dB/div



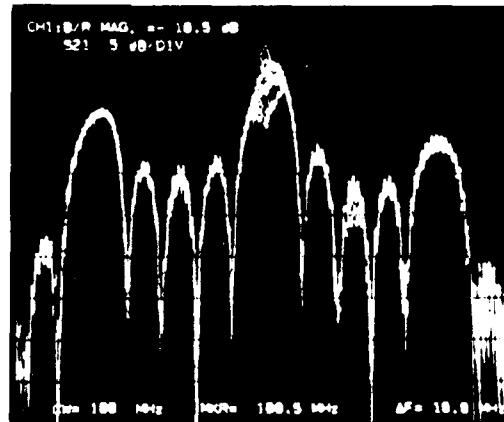
(a) untuned, 0.67MHz/div

5dB/div



(b) tuned, 0.67MHz/div

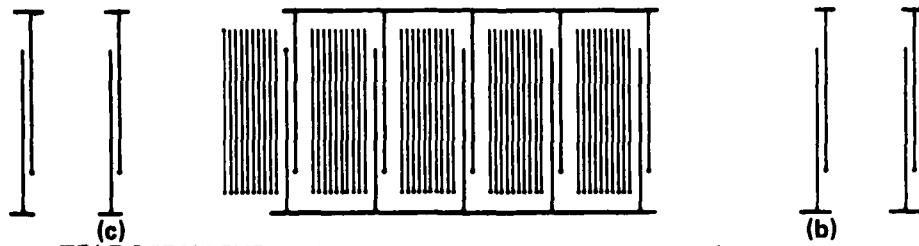
5dB/div



(c) tuned, 3MHz/div

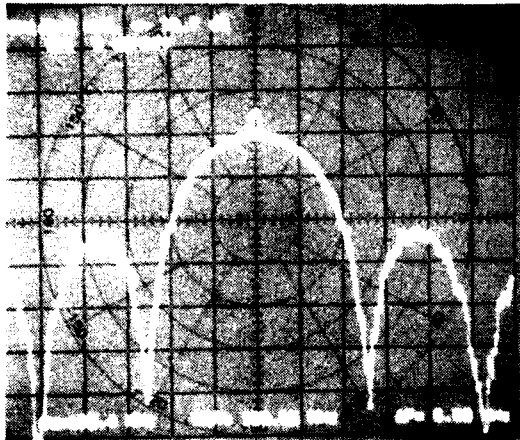
Figure 6. Preliminary measurements on test group-type SPUDT transducer 'A' on YZ-LiNbO<sub>3</sub>.

- (a) shows the forward and reverse responses of the untuned device together with the central trace from the comparison device 'c' without reflectors. The frequency response of the latter is shifted marginally to line up with 'A'.
- (b) shows a similar comparison with input and output transducers series-tuned to match 50  $\Omega$ . This has increased the ripple due to the triple transit signal and caused the upper two traces, each with  $\pm 1$  dB ripple, to almost merge.
- (c) as (b) over a greater bandwidth.

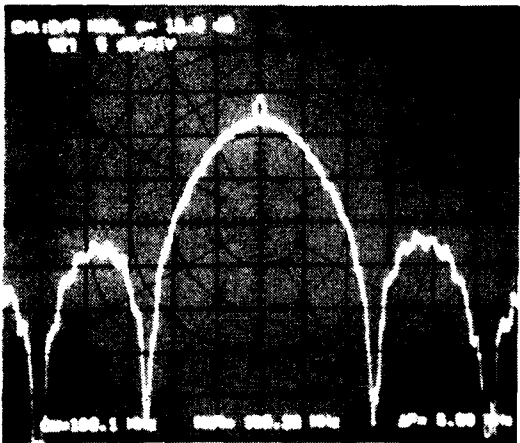
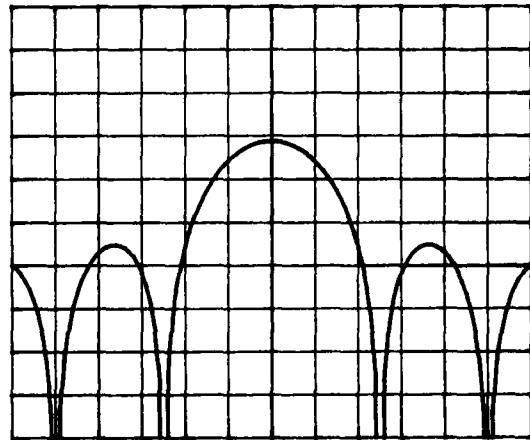


TEST STRUCTURE WITH REFLECTORS DISPLACED  $\lambda/8$  TO RIGHT.

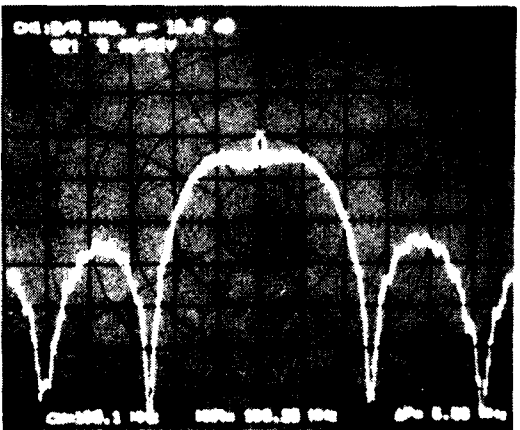
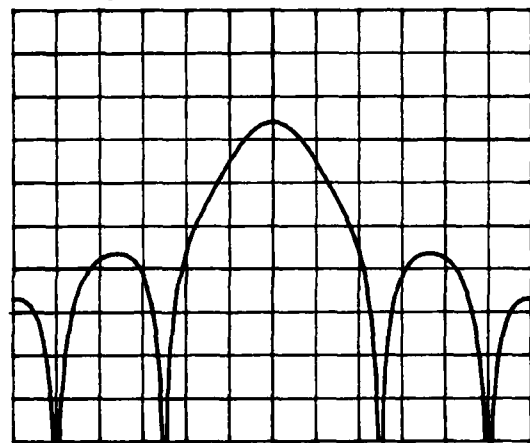
5 dB/div



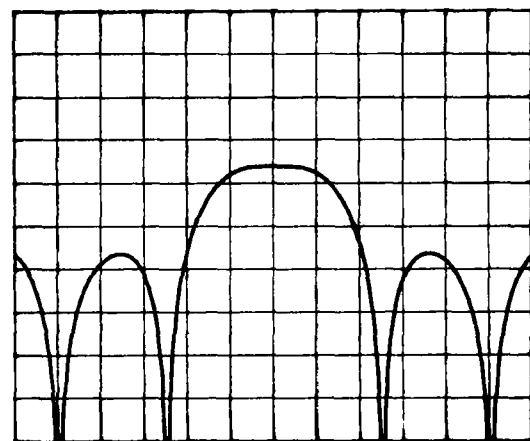
(a) NO REFLECTOR BANKS



(b) SPUDT IN FORWARD DIRECTION

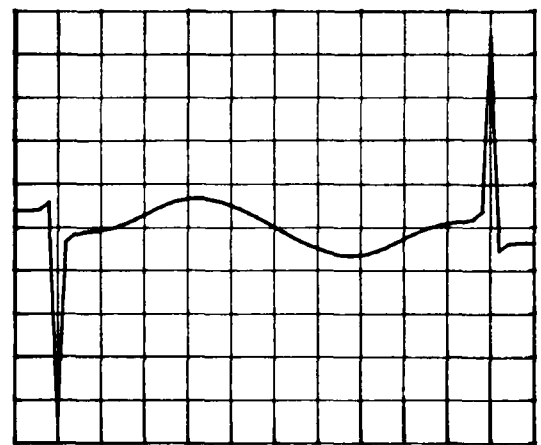
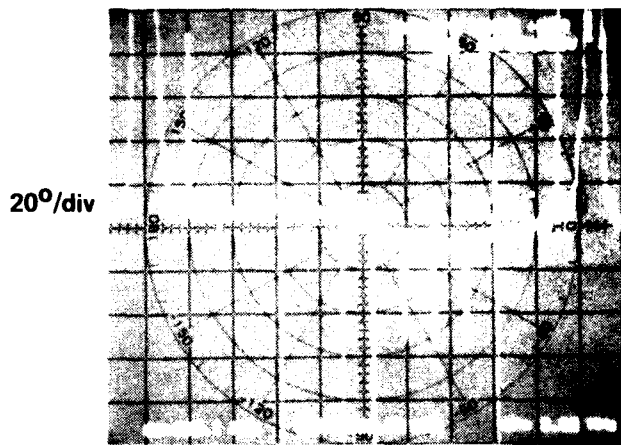
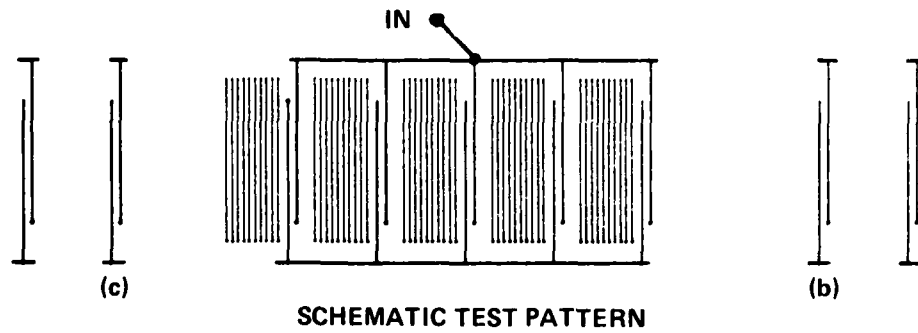


(c) SPUDT IN REVERSE DIRECTION

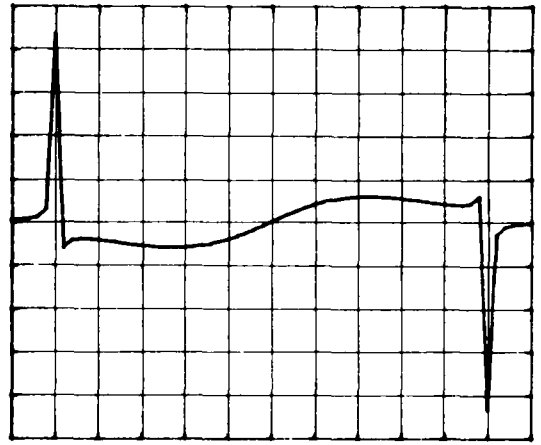
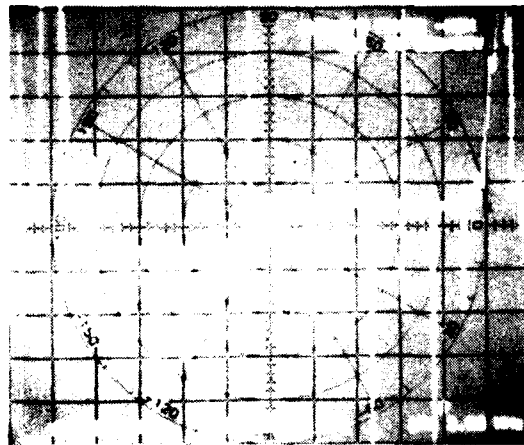


CENTRE FREQUENCY 100 MHz. 1 MHz/div

MEASURED AND CALCULATED RESPONSES OF GROUP-TYPE SPUDT TEST PATTERNS ON Y-Z  $\text{LiNbO}_3$ . THE CENTRAL TRANSDUCER CONTAINS 5 RUNGS OF  $2/3$  SPLIT FINGERS AND OF  $8\lambda$  SPACING. IT IS LOADED WITH A  $10 \Omega$  RESISTOR. (a) NO REFLECTORS. (b) AND (c) REFER TO THE UNTUNED OUTPUT IDT'S IN THE SCHEMATIC, EACH OF WHICH COMPRISES  $5/6$  SPLIT FINGERS. THE TRANSDUCER APERTURES ARE  $100 \lambda$



(b) SPUDT IN FORWARD DIRECTION

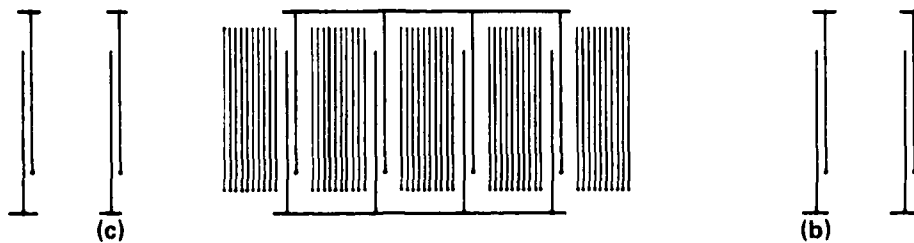


(c) SPUDT IN REVERSE DIRECTION

CENTRE FREQUENCY 100 MHz. 0.5 MHz/div

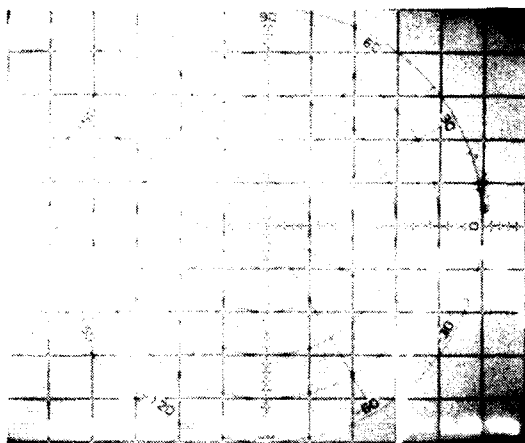
MEASURED AND CALCULATED PHASE DEVIATIONS OF 5-RUNG GROUP-TYPE SPUDT TEST PATTERNS ON Y-Z LiNbO<sub>3</sub>. (b) AND (c) REFER TO THE OUTPUT IDTs IN THE SCHEMATIC, AND THE MEASURED PHASE DEVIATIONS ARE RELATIVE TO DEVICE (a) WITH NO REFLECTORS.

(DEVICES A2 AND C, BK11F, P5) Figure 3

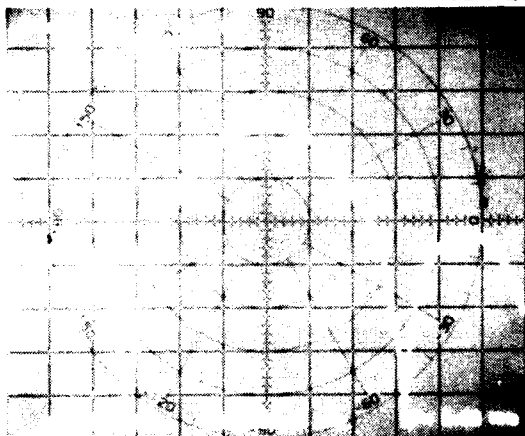
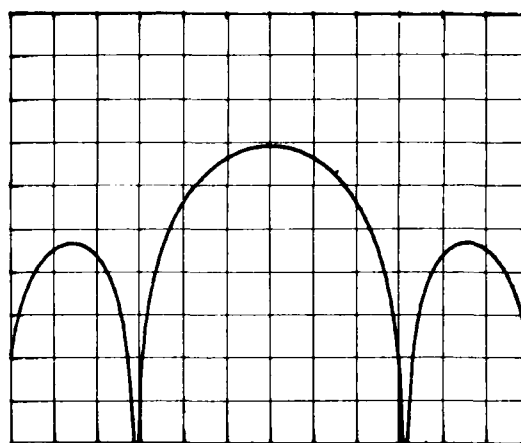


TEST STRUCTURE WITH REFLECTORS DISPLACED  $\lambda/8$  TO RIGHT.

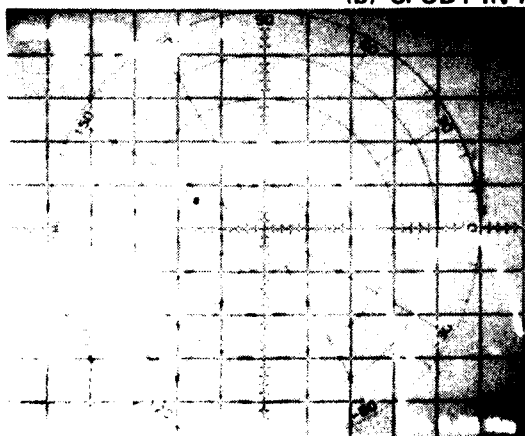
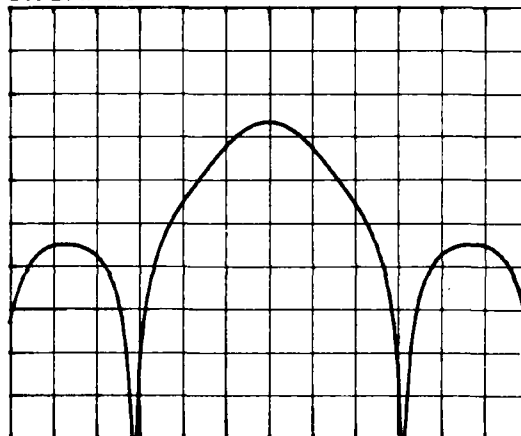
5 dB/div



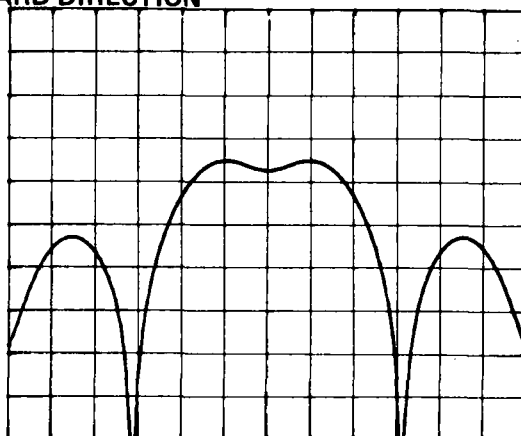
(a) NO REFLECTOR BANKS



(b) SPUDT IN FORWARD DIRECTION

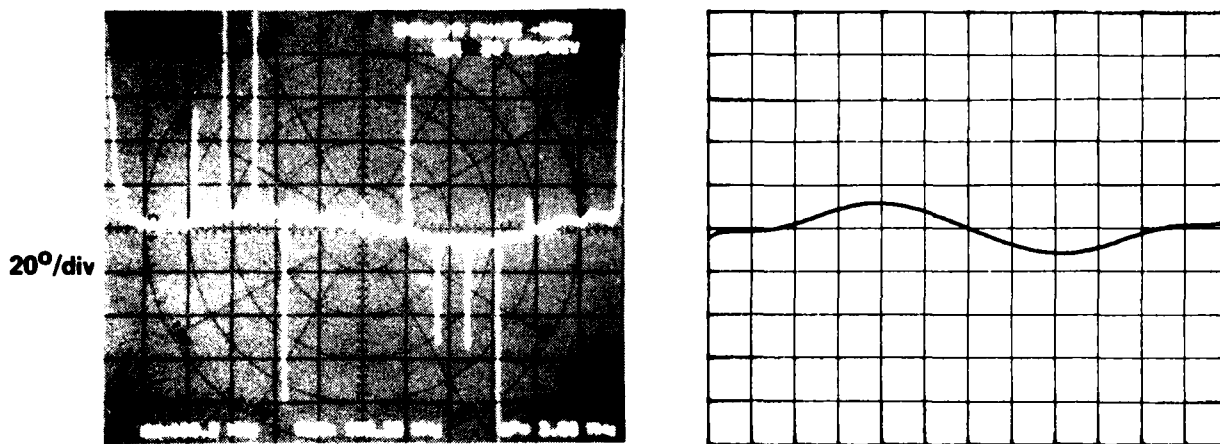
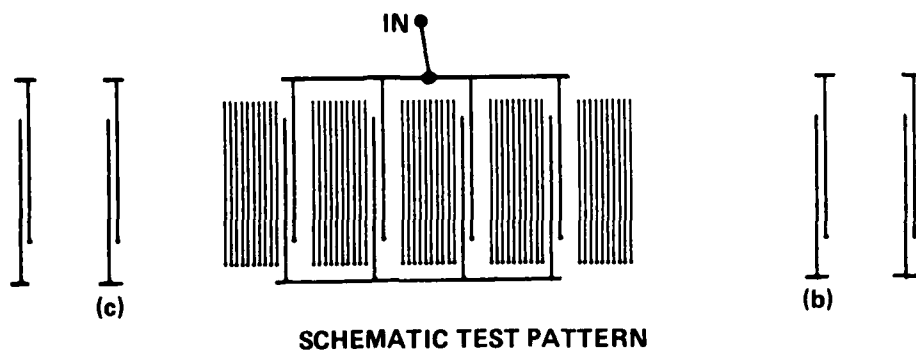


(c) SPUDT IN REVERSE DIRECTION

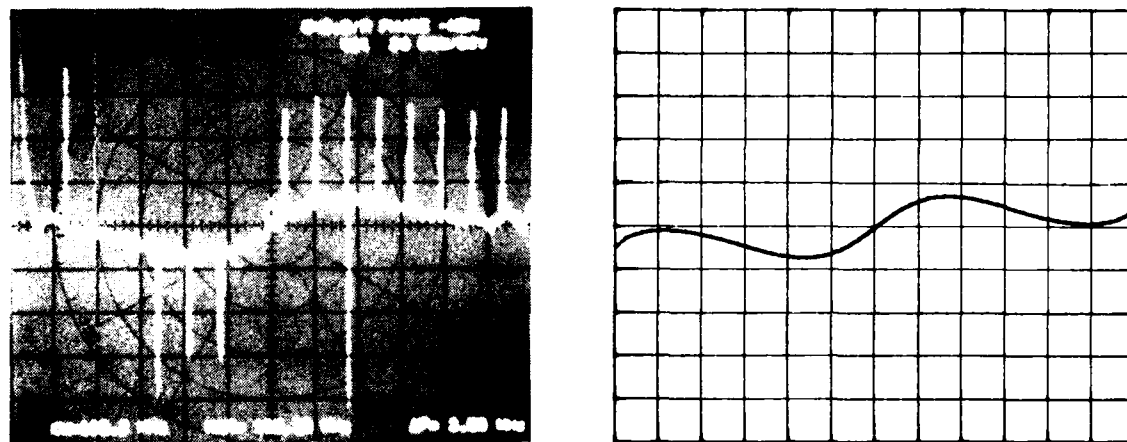


CENTRE FREQUENCY 100 MHz. 1 MHz/div

MEASURED AND CALCULATED RESPONSES OF GROUP-TYPE SPUDT TEST PATTERNS ON Y-Z  $\text{LiNbO}_3$ . THE CENTRAL TRANSDUCER CONTAINS 4 RUNGS OF  $2/3$  SPLIT FINGERS AND OF  $8\lambda$  SPACING. IT IS LOADED WITH A  $10 \Omega$  RESISTOR. (a) NO REFLECTORS. (b) AND (c) REFER TO THE UNTUNED OUTPUT IDT'S IN THE SCHEMATIC, EACH OF WHICH COMPRISES  $5/6$  SPLIT FINGERS. THE TRANSDUCER APERTURES ARE  $100 \lambda$



(b) SPUDT IN FORWARD DIRECTION



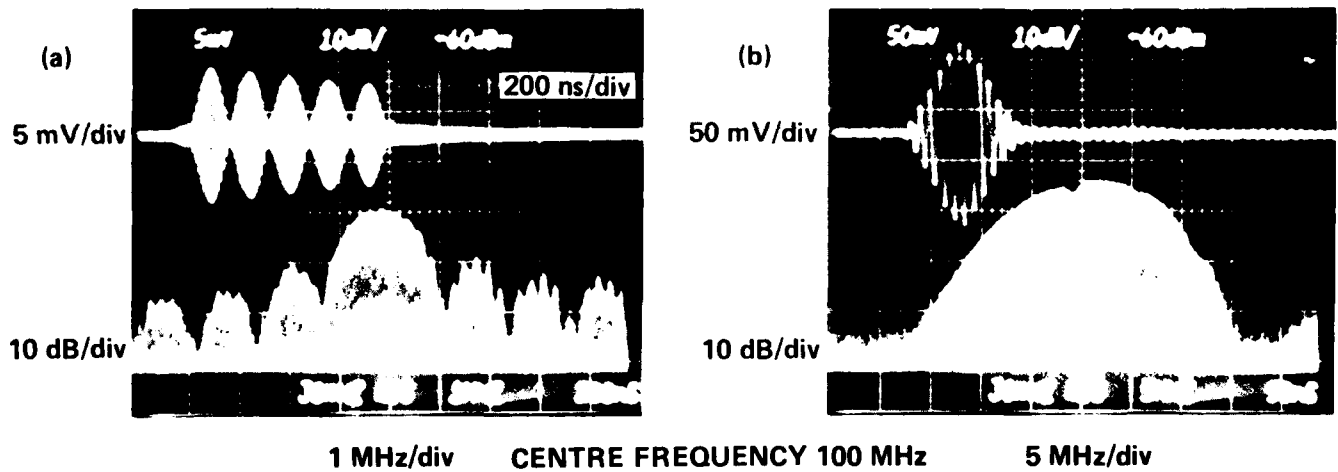
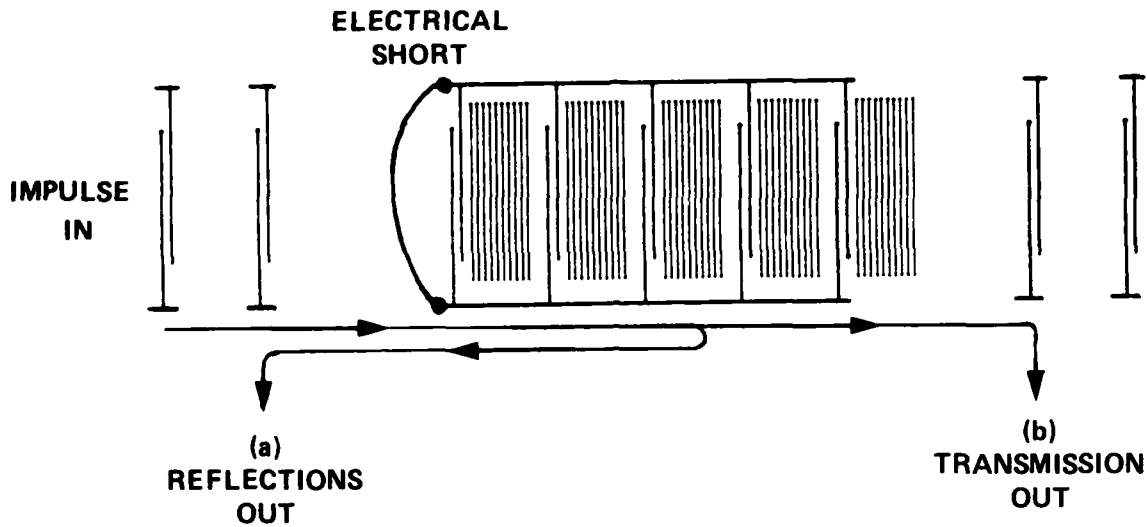
(c) SPUDT IN REVERSE DIRECTION

CENTRE FREQUENCY 100 MHz. 0.5 MHz/div

MEASURED AND CALCULATED PHASE DEVIATIONS OF 4-RUNG GROUP-TYPE SPUDT TEST PATTERNS ON Y-Z  $\text{LiNbO}_3$ . (b) AND (c) REFER TO THE OUTPUT IDTs IN THE SCHEMATIC, AND THE MEASURED PHASE DEVIATIONS ARE RELATIVE TO DEVICE (a) WITH NO REFLECTORS.

(DEVICES A2 AND C, BK11F, P5) Figure 10

**SCHEMATIC OF SPUDT REFLECTION COEFFICIENT MEASUREMENTS**



REFLECTION COEFFICIENT MEASUREMENT AND FREQUENCY RESPONSE. WHEN THE LEFT HAND SIDE IDT IS IMPULSED THE ENERGY REFLECTED IS MEASURED ON OUTPUT (a), AND THAT TRANSMITTED ON OUTPUT (b). COMPARISON YIELDS AN AMPLITUDE REFLECTION COEFFICIENT PER REFLECTOR BANK OF APPROX 0.12. A LOW-PASS FILTER REJECTS THE THIRD HARMONIC CONTENT OF THESE SPLIT-FINGER DEVICES.

(BK 11F, p17, DEVICE A) Figure 11

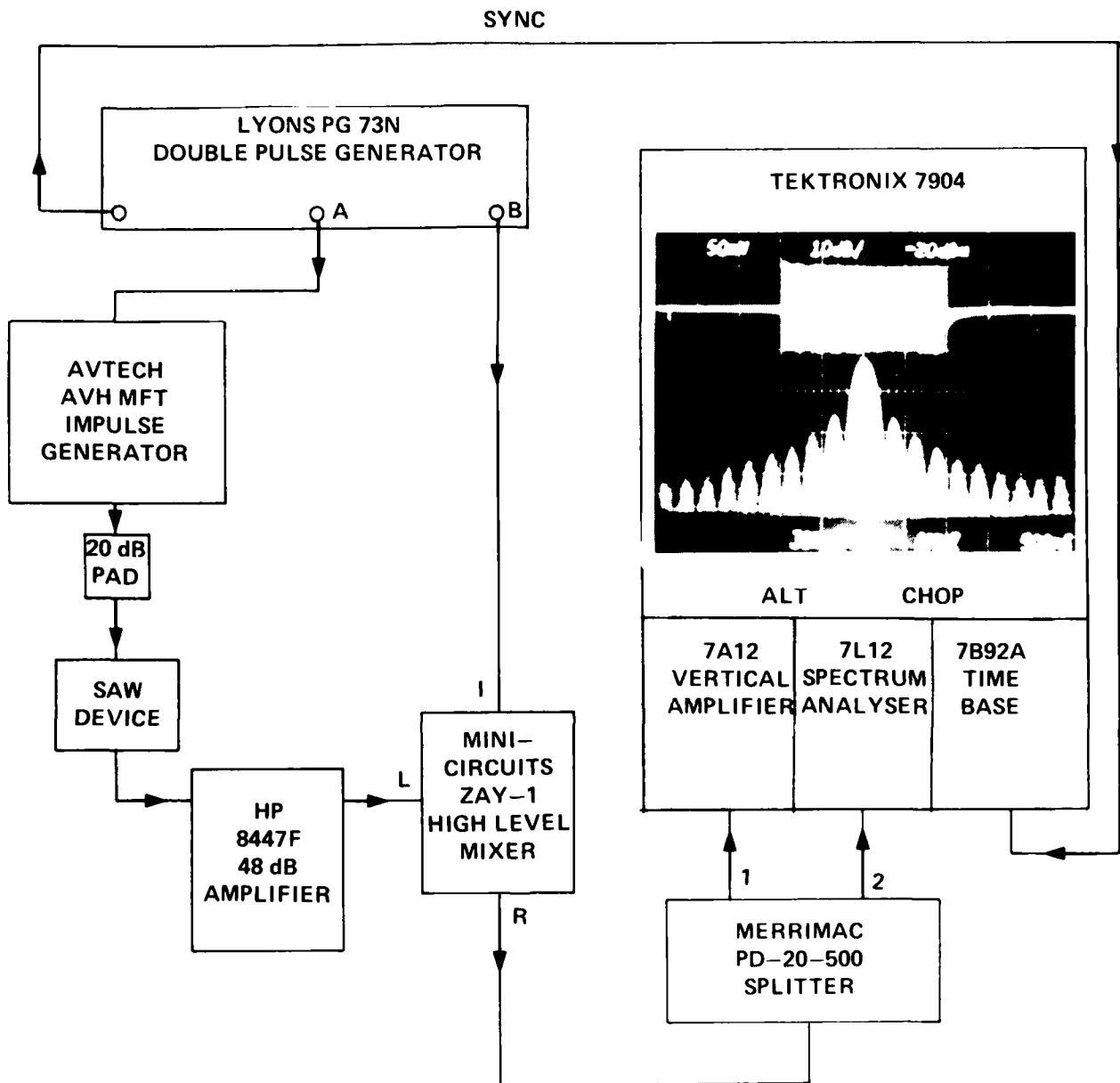
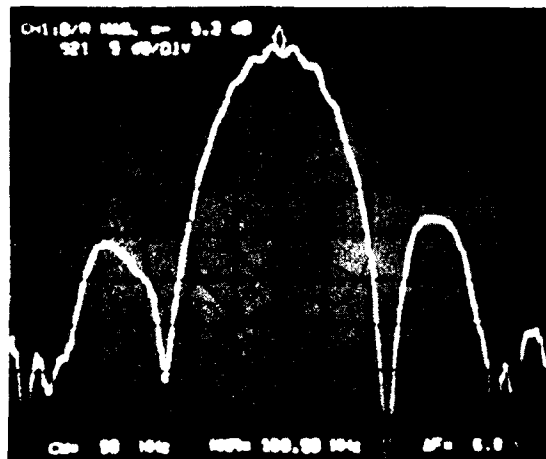


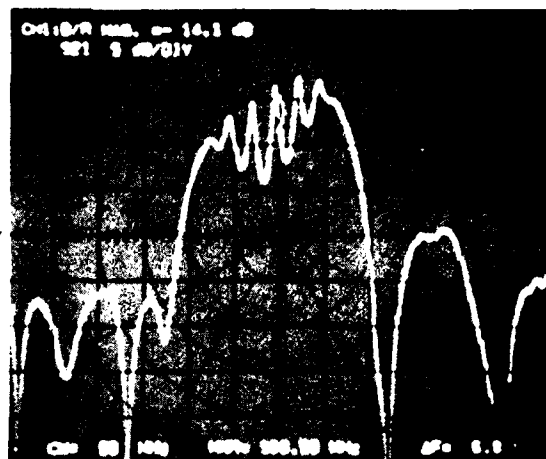
FIGURE 12. Schematic time-domain and frequency-domain measurement system at RSRE. The double pulse generator has two outputs, A and B, whose widths and relative delay are variable at will. Output A impulses the device and provides a simultaneous display of the impulse response and the frequency response, as shown in the photograph. Output B operates a high-level mixer, and may be used to remove parts of the impulse response for diagnostic or design purposes (FROM: MFL Book 54 p. 237).

5dB/div



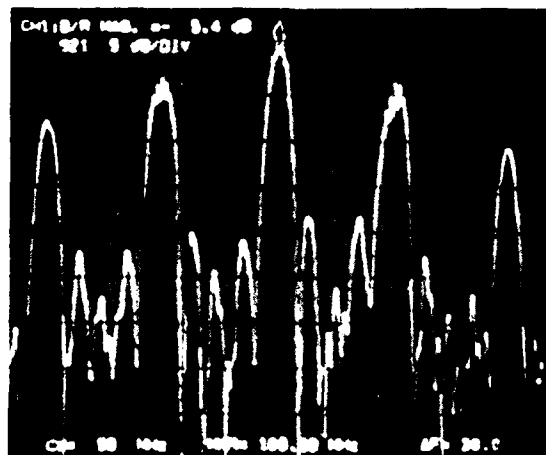
(a) 1MHz/div

5dB/div



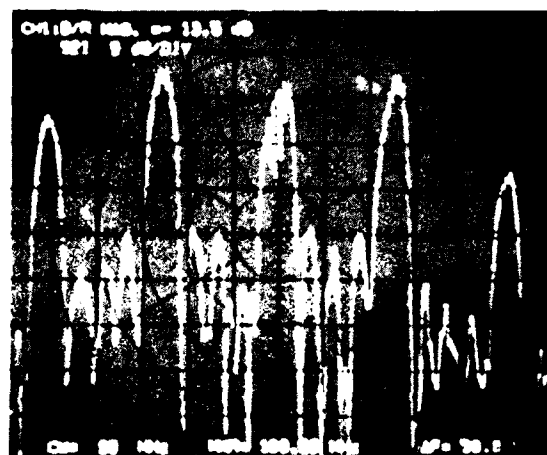
(d) 1MHz/div

5dB/div

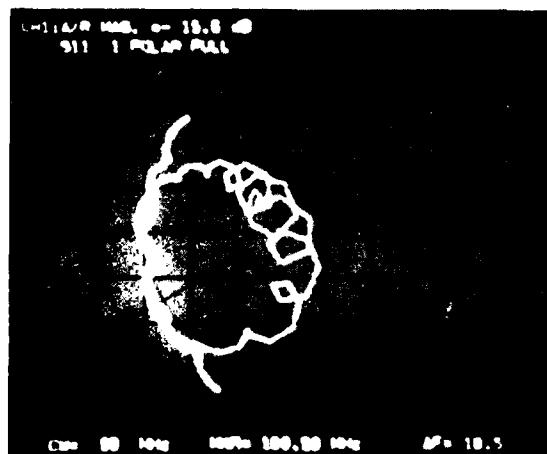


(b) 5MHz/div

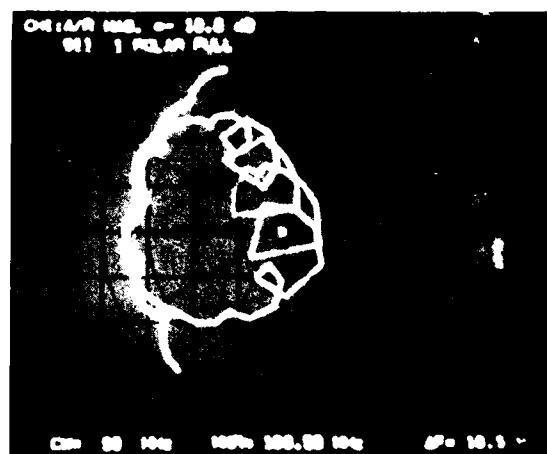
5dB/div



(e) 5MHz/div



(c)



(f)

Figure 13. Detailed measurements on SPUDT devices comprising two transducers 'A', each series-tuned.

(a), (b) and (c) refer to the forward pair, the  $S_{11}$  measurement in (c) being made with the other transducer tuned and loaded with  $50\Omega$ .

(d), (e) and (f) are the corresponding responses of the reverse pair of transducers

(FROM MFL Book 11F, p81)

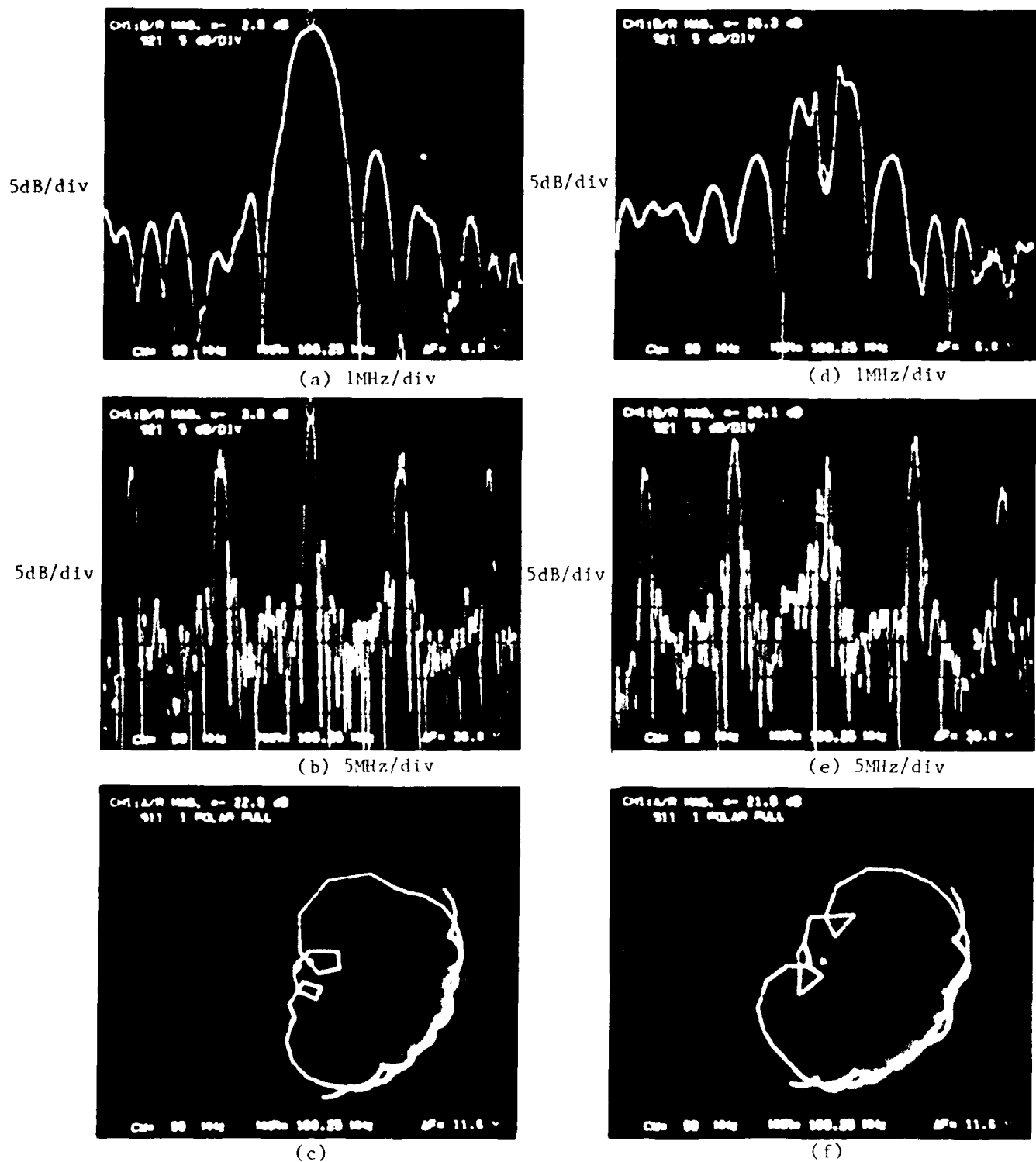
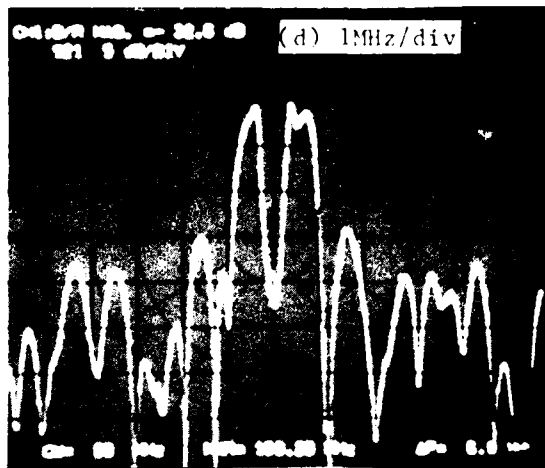
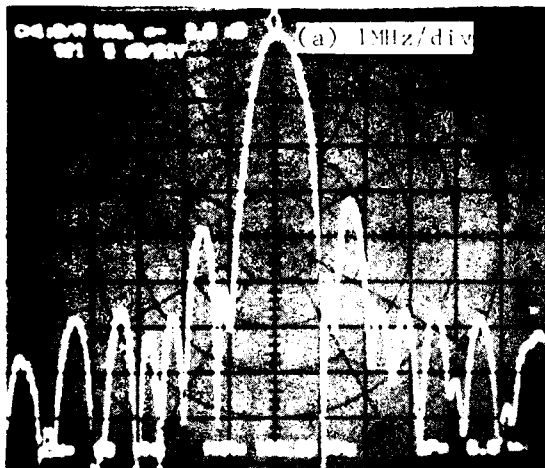


Figure 14. Detailed measurements on SPUDT devices comprising 2 transducers 'D', each shunt-tuned.

(a), (b) and (c) refer to the forward pair, the  $S_{11}$  measurement in (c) being made with the other transducer tuned and loaded with  $50\Omega$ .

(d), (e) and (f) are the corresponding responses of the reverse pair of transducers.

5dB/div



5dB/div

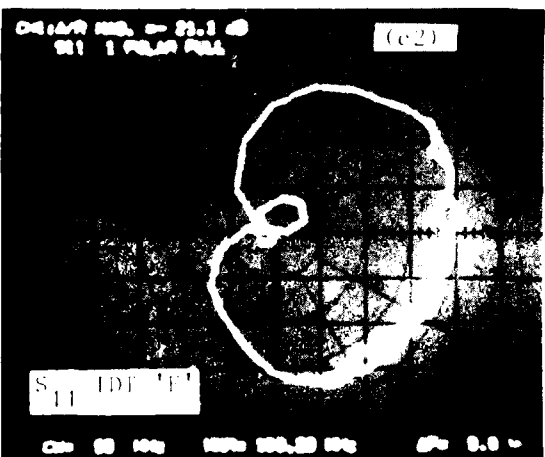
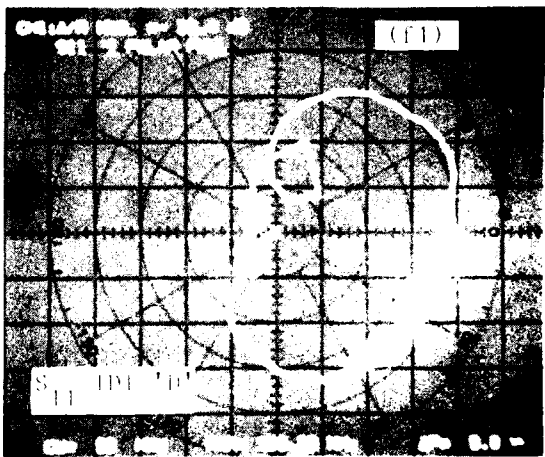
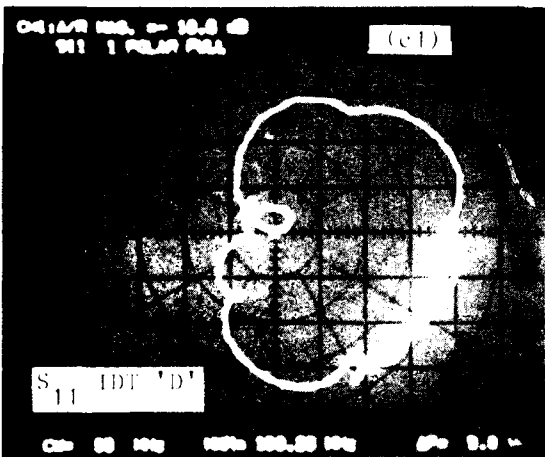
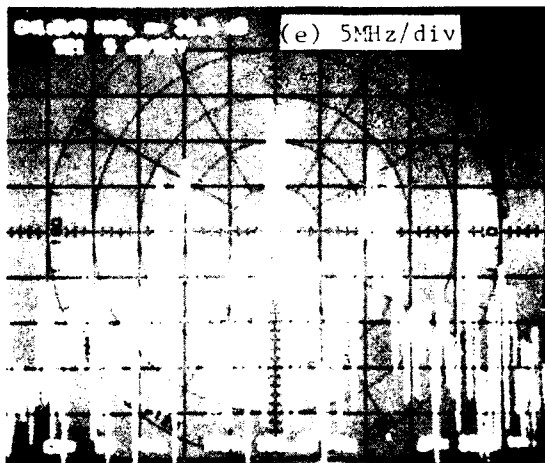
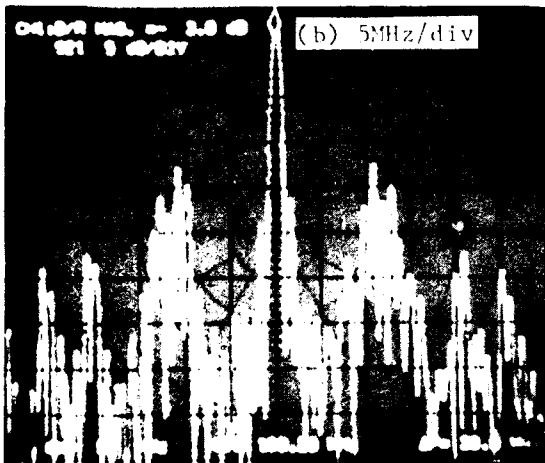
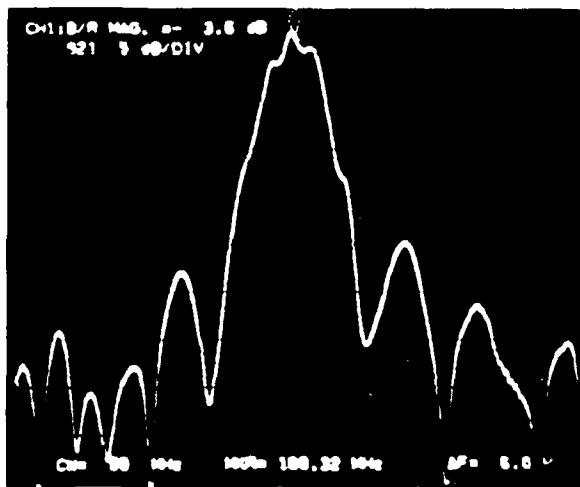
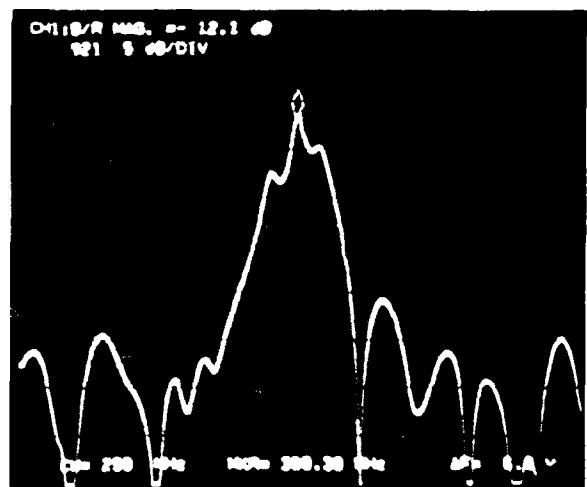


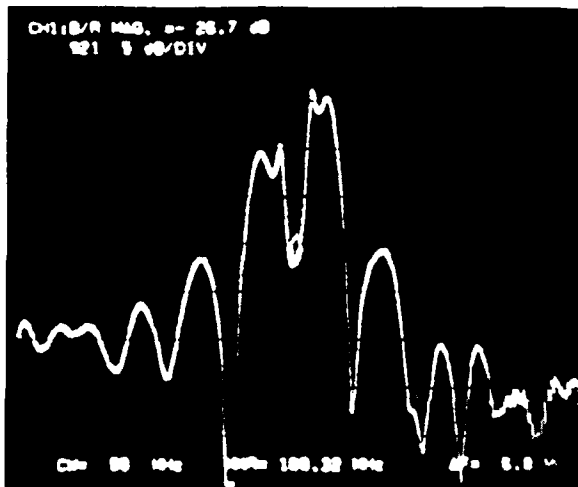
Figure 15. Detailed measurements on SPUDT devices comprising transducers 'D' and 'E', each shunt tuned. (a),(b) and (c) refer to the forward pair, and (d), (e) and (f) to the reverse pair. In each  $S_{11}$  measurement the other IDT is tuned and loaded with  $50\Omega$ . (From: M.F.L. Book 11F, p.81).



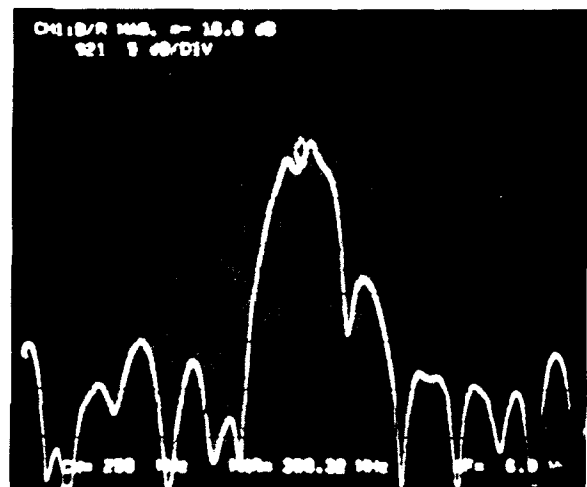
(a)



(b)



(c)



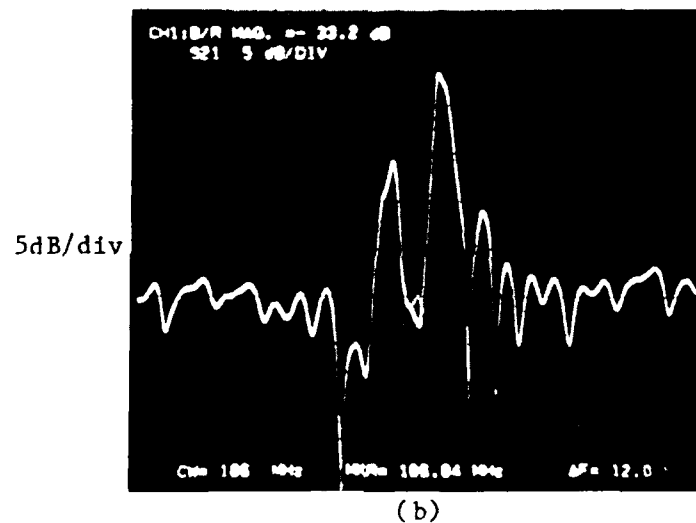
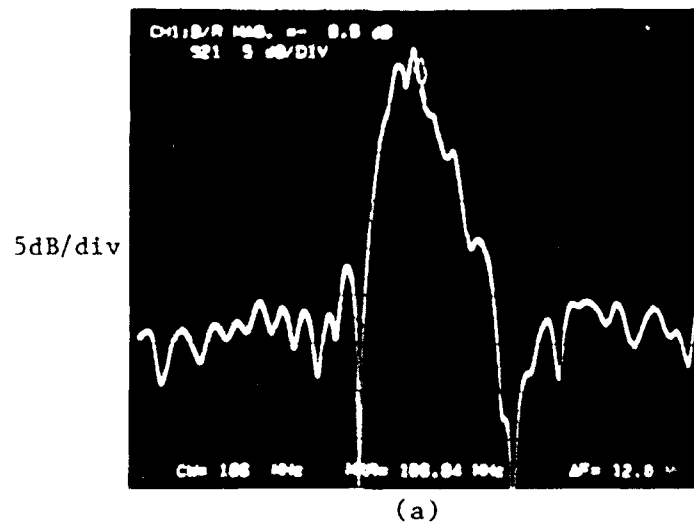
(d)

Vertical scales: 5 dB/div throughout

Figure 16. A comparison of group-type SPUDT devices employing two transducers 'D' untuned at their fundamental and third harmonics.

- (a) forward pair at 100 MHz, 1 MHz/div
- (b) same pair at 300 MHz, 1 MHz/div
- (c) reverse pair at 100 MHz, 1 MHz/div
- (d) same pair at 300 MHz, 1 MHz/div

(FROM MFL Book 11F, pp 89-91)

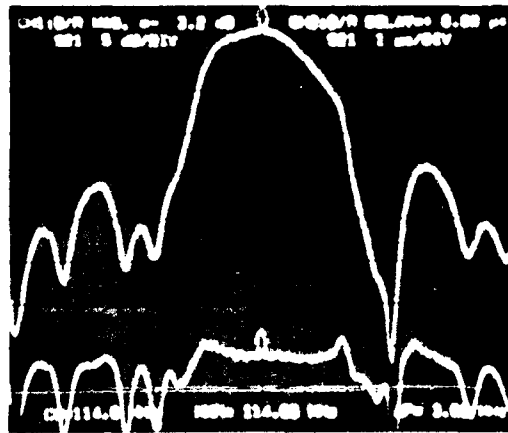


centre frequency 186.85MHz, 2MHz/div

Figure 17. Responses of group-type SPUDT devices employing untuned transducers 'D' and 'E' with shorted reflector banks from modified mask AW 1728/M (MFL Book 11D, p28)

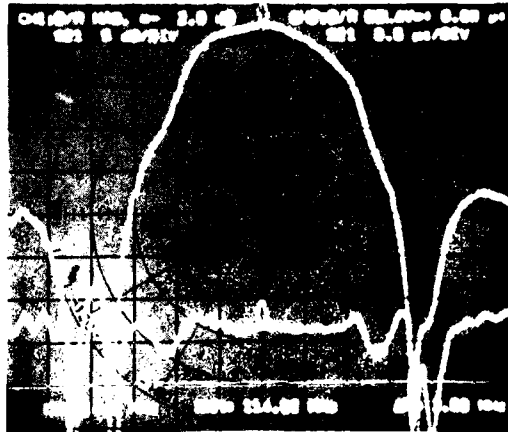
- (a) shows the response in the forward direction for a device with isolated reflectors. Note: reflector banks  $\lambda/8$  away from other transducer.
- (b) shows the response in the reverse direction for a device with isolated reflectors. Note: reflector banks  $\lambda/8$  towards other transducer.

5dB/div



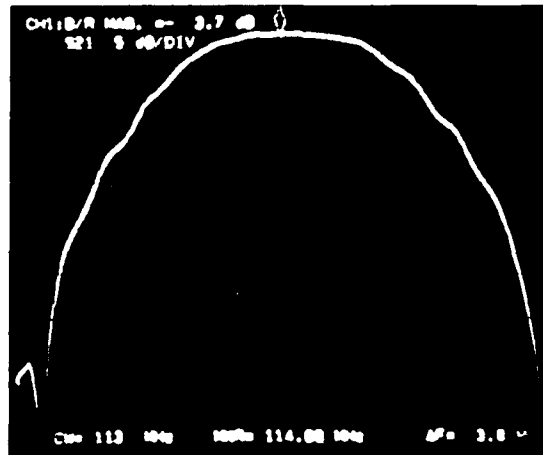
(a)

5dB/div



(b)

5dB/div



(c)

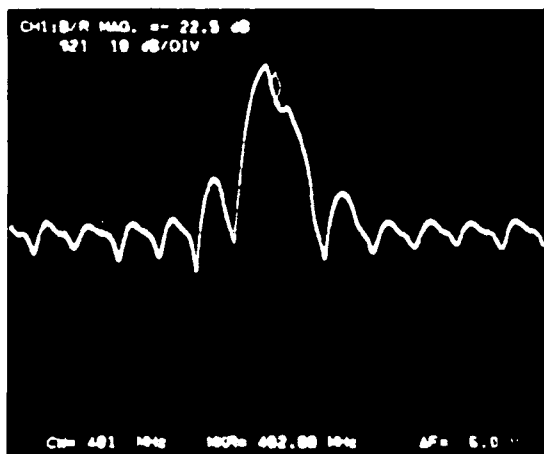
centre frequency 114MHz, 0.5 MHz/div

Figure 18. Measurements on group-type SPUDT devices on  $128^\circ \text{LiNbO}_3$ .

- (a) response of a device comprising transducers 'D' and 'E' each shunt-tuned.
- (b) response of the same device reduced to 7 rungs per transducer and retuned.
- (c) response of a device comprising two transducers 'A' matched to  $50\Omega$  through shunt/series tuning.

(FROM MFL Book 11D pp23-6)

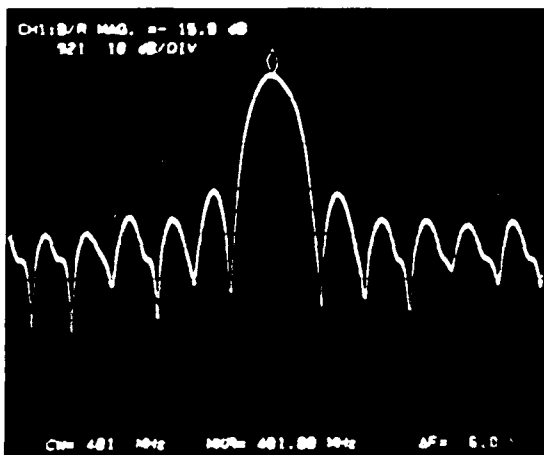
10dB/div



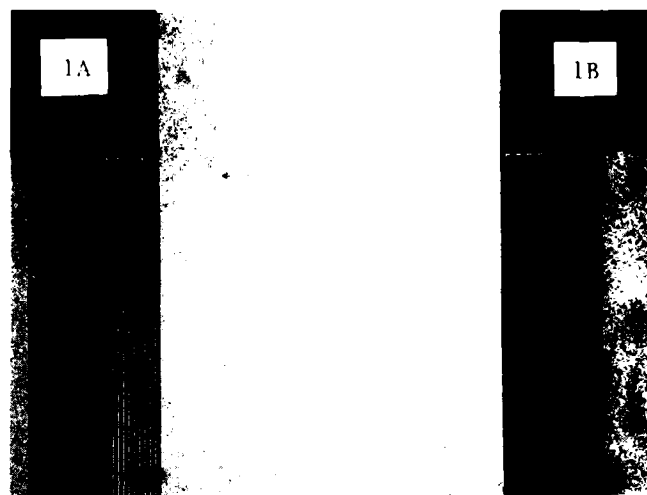
(a) 1MHz/div



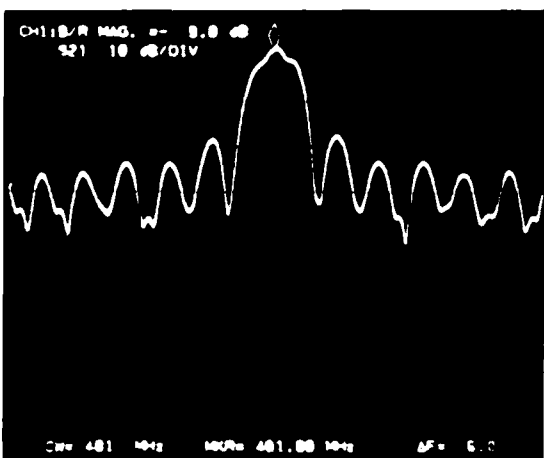
(d) transducer 1A



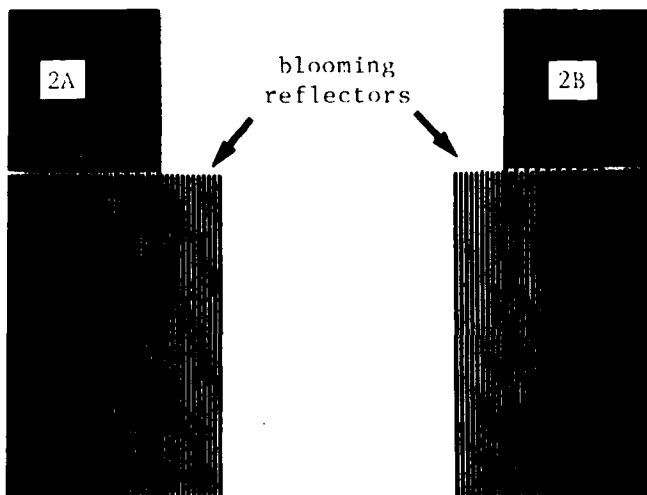
(b)



(e)



(c)



(f)

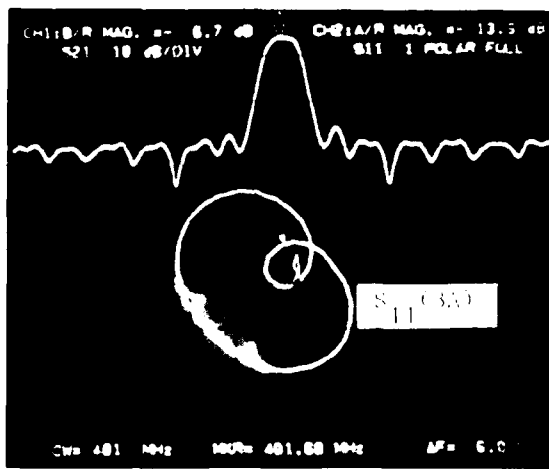
centre frequency,  $\sim 400$  MHz. 1MHz/div

Figure 19. Measurements on ST-quartz devices

- (a) shows the response of untuned pattern '1'
- (b) shows the response of untuned pattern '2', with blooming
- (c) shows the response of pattern '2' tuned and matched to  $50 \Omega$
- (d) shows the structure of transducer 1A
- (e) shows a close-up of the nearest approach of transducers 1A and 1B
- (f) shows a similar close-up of pattern '2' with blooming

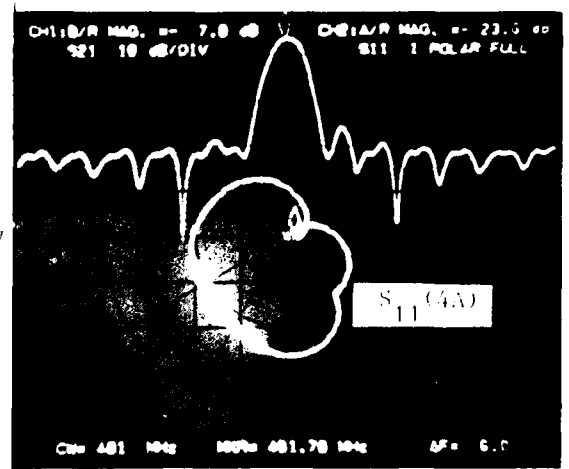
(FROM MFL Book 11F, p67)

10dB/div



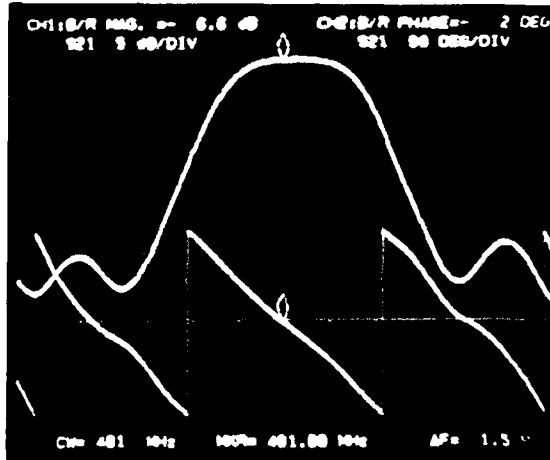
1MHz/div

10dB/div



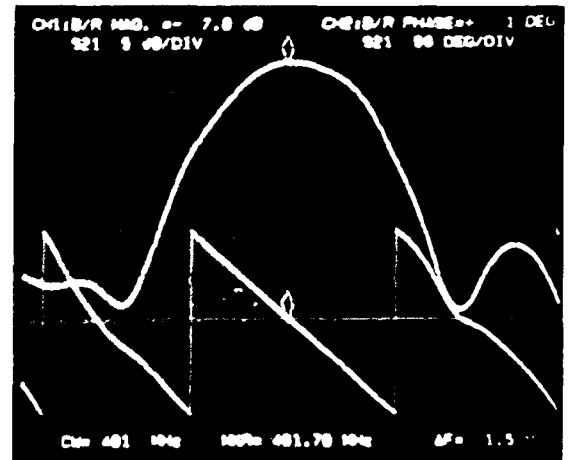
1MHz/div

5dB/div



0.25MHz/div

5dB/div



0.25 MHz/div

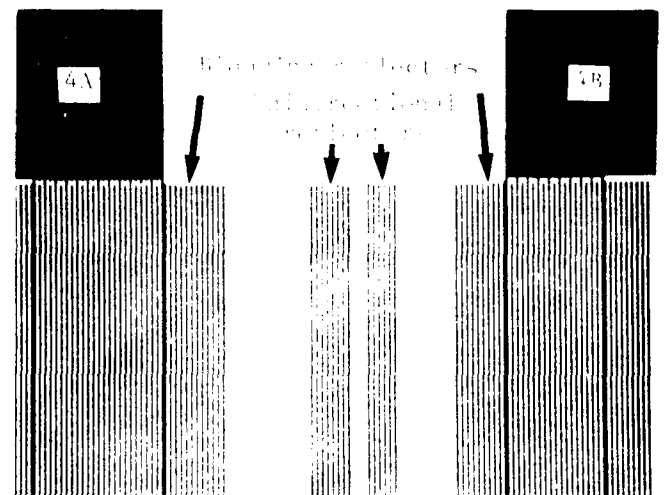
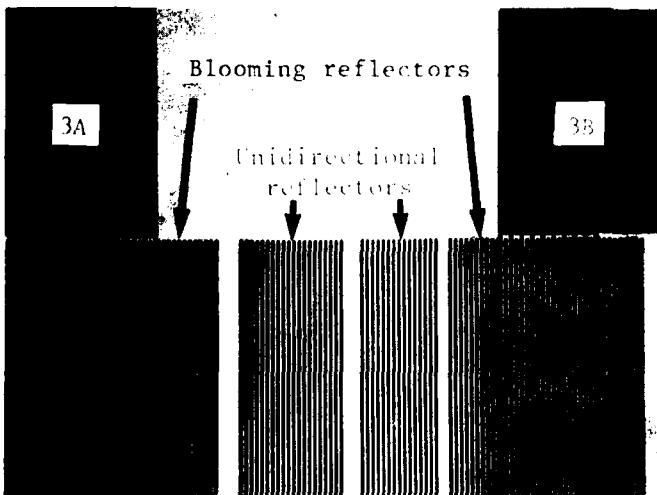
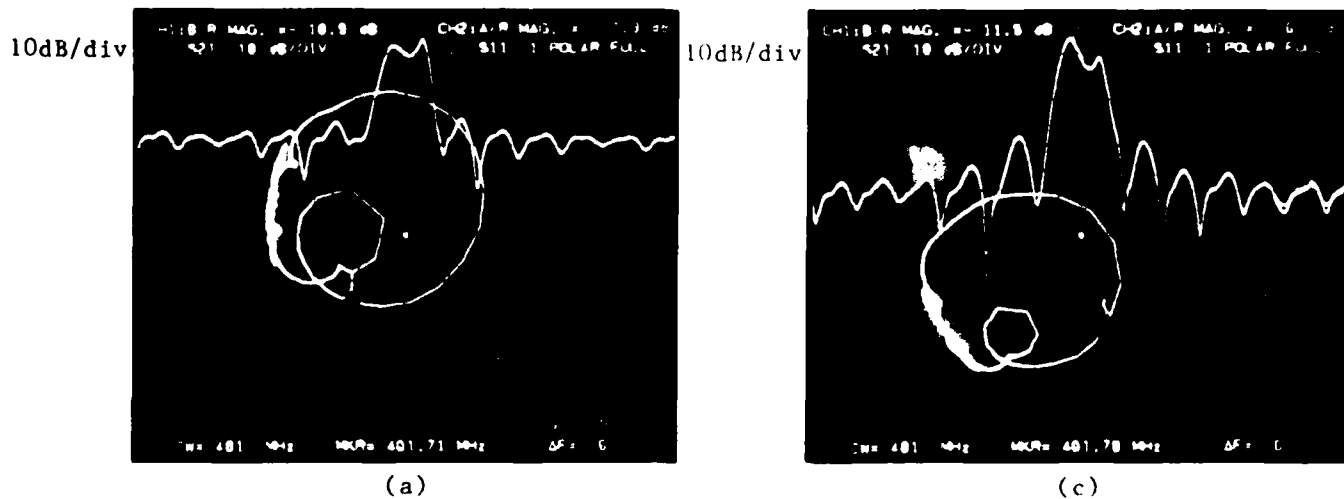


Figure 20. Measurements on SPUDT patterns '3' and '4' on ST-quartz.

- (a) and (b) show the response of matched devices of pattern '3'
- (c) shows a close-up of the nearest approach of transducers 3A and 3B
- (d) and (e) show the response of matched devices of pattern '4'
- (f) shows a close-up of the nearest approach of transducers 4A and 4B

(FROM MFL Book 11F p 69)



centre frequency, 400MHz. 1MHz/div

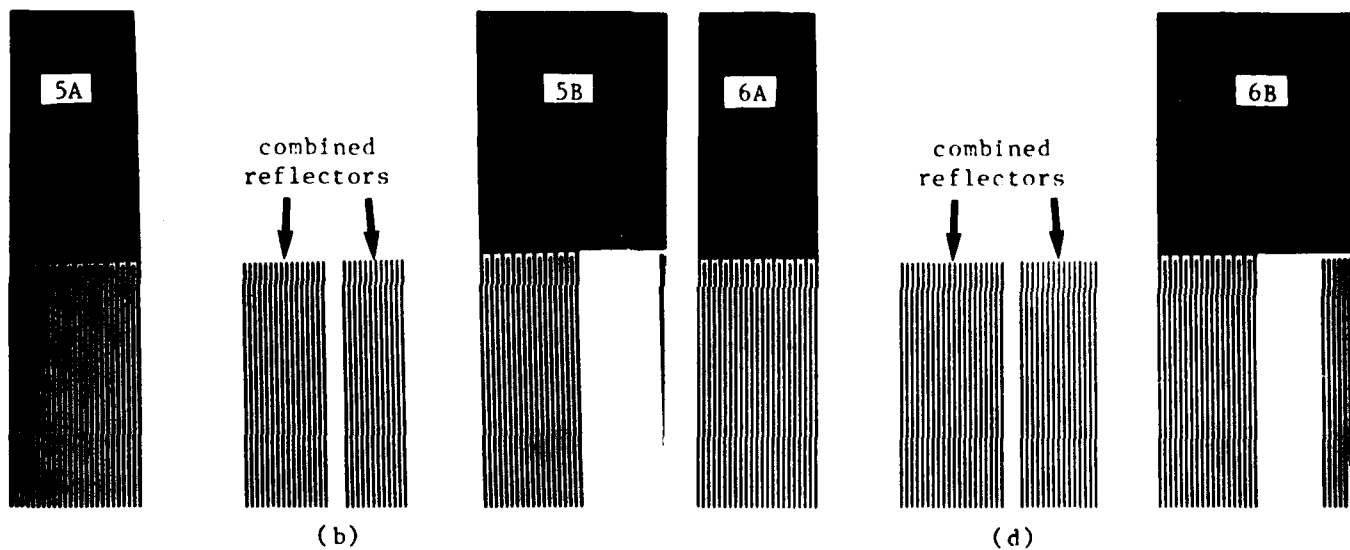
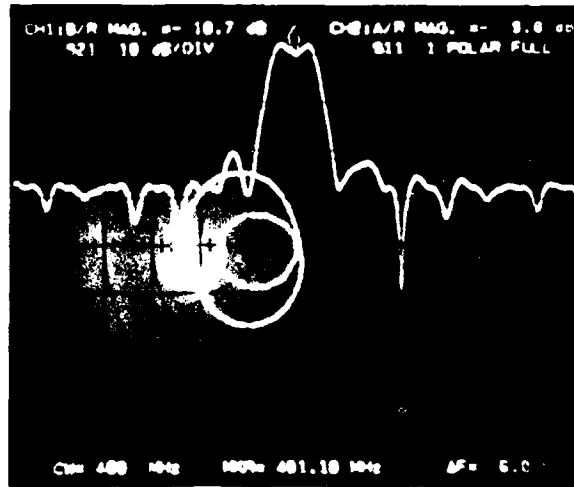


Figure 21. Measurements on patterns '5' and '6' which attempted to combine the blooming and unidirectional reflections.

- (a) response of matched device '5' including  $S_{11}$  of transducer 5A
- (b) close-up of nearest approach of transducers 5A and 5B
- (c) response of matched device '6' including  $S_{11}$  of transducer 6A
- (d) close up of nearest approach of transducers 6A and 6B

(FROM MFL Book 11F, p 71)

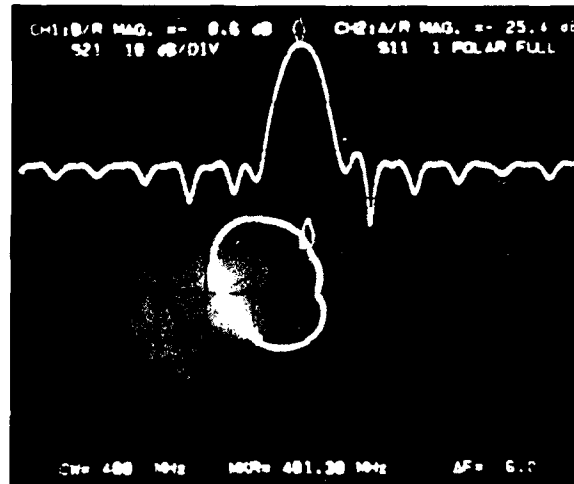
10dB/div



(a)

1MHz/div

10dB/div



(b)

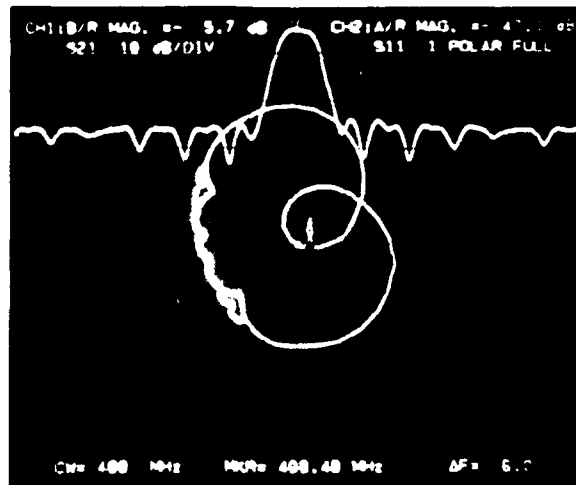
1MHz/div

Figure 22. Measurements on SPUDT devices employing  $1500 \text{ \AA}$  Al on ST-quartz.

- (a) response of matched pattern '3' including  $S_{11}$  of transducer 3A
- (b) response of matched pattern '4' including  $S_{11}$  of transducer 4A

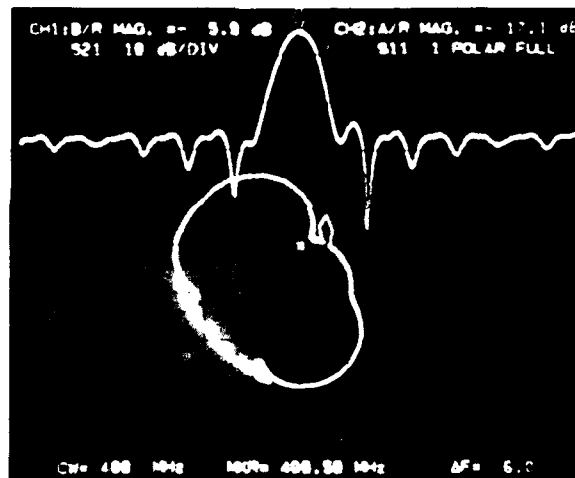
(FROM MFL Book 11F p 73)

10dB/div



(a)

10dB/div



(b)

centre frequency 400MHz 1MHz/div

Figure 23. Measurements on SPUDT devices employing  $900\text{\AA}$  Al on AT-quartz (with SAW propagation along the x-axis)

- (a) response of matched pattern '3' including  $S_{11}$  of transducer 3A
- (b) response of matched pattern '4' including  $S_{11}$  of transducer 4A

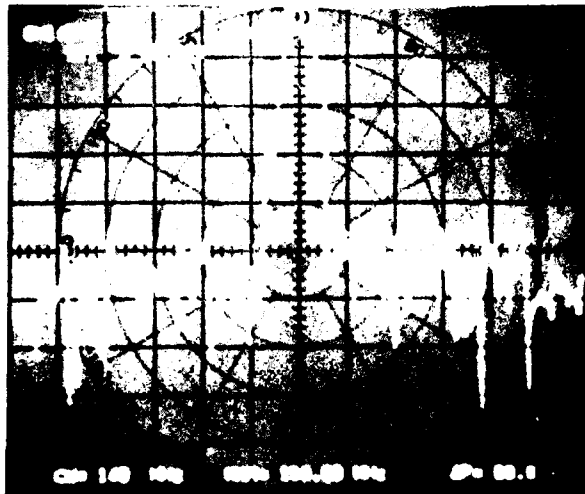
(FROM MFL Book 11F p 65)

Pattern	Number of rungs in IDT A	Number of F/P per rung	Blooming	Unidirectional reflectors	Number of rungs in IDT B	Number of F/P per rung	Blooming	Unidirectional reflectors
1	9 (rung-to-rung separation $48\lambda$ )	12 (12/13 fingers)	-	-	12 (rung-to-rung separation $36\lambda$ )	9 (9/10 fingers)	-	-
2	9	12	Yes moved $\lambda/4$ towards fingers	-	12	9	Yes moved $\lambda/4$ towards fingers	-
3	9	12	Yes	40 reflectors per period. Offset $\lambda/8$ away from other transducer	12	9	Yes	30 reflectors per period. Offset $\lambda/8$ away from other transducer
4	9	12	Yes	16 reflectors per period. Offset $\lambda/8$ away from other transducer	12	9	Yes	12 reflectors per period. Offset $\lambda/8$ away from other transducer
5	9	12	Combined into 40 reflectors per period. Offset $0.18\lambda$ away from other transducer.		12	9	Combined into 30 reflectors per period. Offset $0.18\lambda$ away from other transducer.	
6	9	12	Combined into 32 reflectors per period. Offset $0.197\lambda$ away from other transducer.		12	9	Combined into 24 reflectors per period. Offset $0.197\lambda$ away from other transducer.	

Patterns AW1729. All apertures:  $100\lambda$ .  $\lambda = 7.855 \mu\text{m}$ . M F Lewis Bk 11c p.34

TABLE 1

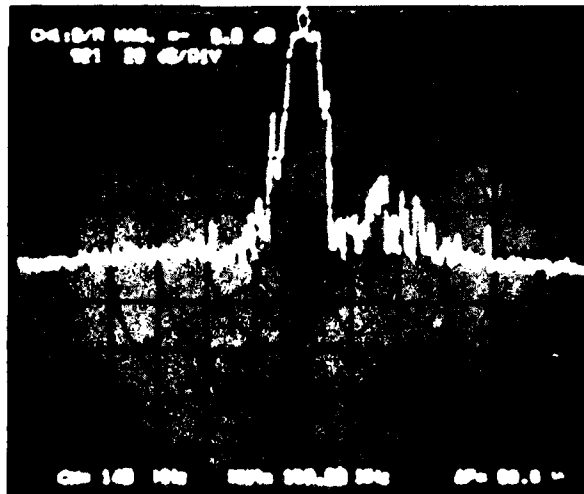
5 dB/div



ONE IIDT-4 DEVICE ON YZ-LiNbO<sub>3</sub>

CENTRE FREQUENCY, 150 MHz. 10 MHz/div

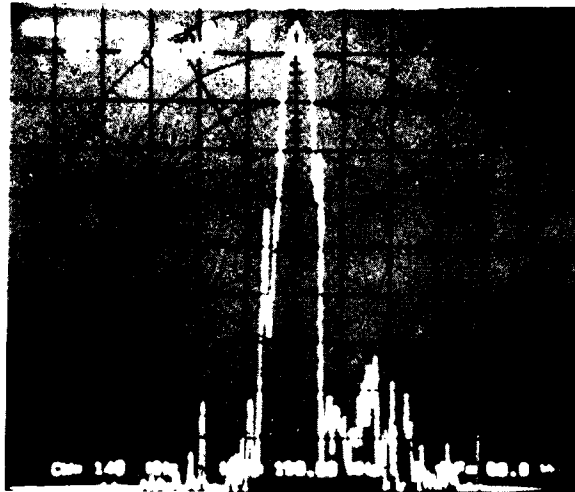
20 dB/div



FOUR IIDT-4 DEVICES IN SERIES

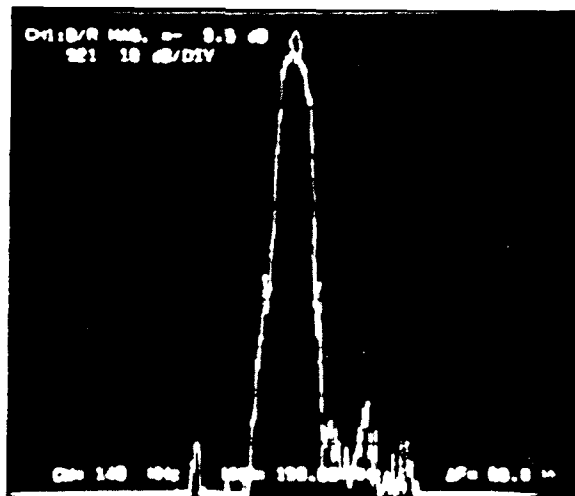
Figure A1. A comparison of the frequency response of one low-loss (IIDT) SAW device with that of 4 such devices in series. The IIDT-4 device is described in reference 8. (From: MFL Book 48, page 34).

10 dB/div



**FOUR IIDT DEVICES IN SERIES**  
**CENTRE FREQUENCY, 150 MHz 10 MHz/div**

10 dB/div



**AS ABOVE BUT WITH TWO DEVICES**  
**HEATED TO PROVIDE 'STAGGER-TUNING'**

Figure A2. A demonstration that low-loss SAW technology can lead to improved out-of-band rejection and an acceptable insertion loss. The upper figure reproduces the lower measurement of Figure A1 on a conventional scale (10 dB/div). In the lower figure the responses of the devices have been staggered by heating two of them. This reduces the cumulative effect of imperfections in the individual designs.

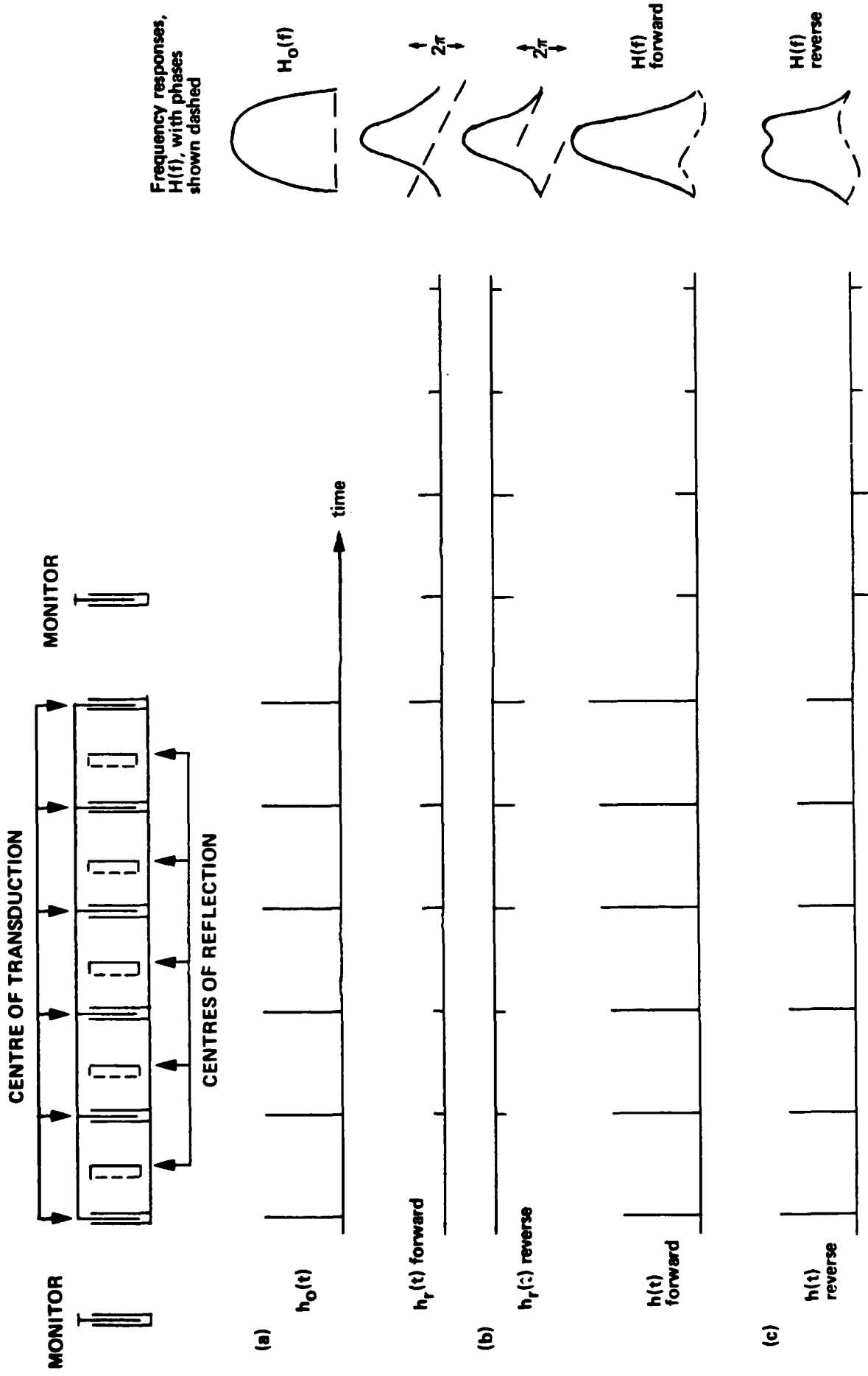


Figure A3. (a) Schematic SPUDT transducer containing  $N = 6$  rungs with  $\delta$  - function reflectors between the rungs. The impulse response of the transducer fingers alone is  $h_0(t)$  with frequency response  $H_0(f)$ . (b) Impulse response of the reflectors,  $h_r(t)$ , in the forward and reverse directions. (c) Overall impulse responses,  $h(t)$ , and frequency responses,  $H(f)$ , in the forward and reverse directions.

## DOCUMENT CONTROL SHEET

Overall security classification of sheet ..... UNCLASSIFIED .....

(As far as possible this sheet should contain only unclassified information. If it is necessary to enter classified information, the box concerned must be marked to indicate the classification eg (R) (C) or (S) )

1. DRIC Reference (if known)	2. Originator's Reference MEMORANDUM 3833	3. Agency Reference	4. Report Security U/C Classification	
5. Originator's Code (if known)	6. Originator (Corporate Author) Name and Location ROYAL SIGNALS AND RADAR ESTABLISHMENT			
5a. Sponsoring Agency's Code (if known)	6a. Sponsoring Agency (Contract Authority) Name and Location			
7. Title A STUDY OF GROUP-TYPE SINGLE-PHASE UNIDIRECTIONAL SAW TRANSDUCERS ON LiNbO <sub>3</sub> AND QUARTZ				
7a. Title in Foreign Language (in the case of translations)				
7b. Presented at (for conference papers) Title, place and date of conference				
8. Author 1 Surname, initials LEWIS M F	9(a) Author 2	9(b) Authors 3,4...	10. Date	pp. ref.
11. Contract Number	12. Period	13. Project	14. Other Reference	
15. Distribution statement UNLIMITED				
Descriptors (or keywords)				
continue on separate piece of paper				
Abstract This Memorandum describes a development of the SPUDT (Single Phase Unidirectional Transducer) concept. The fabrication of such devices requires a single stage of photolithography. Prototype devices have shown very encouraging passband characteristics with an insertion loss of less than 3 dB on LiNbO <sub>3</sub> at 100 MHz, and less than 6 dB on quartz at 400 MHz. In each case the amplitude response is essentially ripple-free, and the phase characteristic agreeable linear.				

DTIC

END

4-86